Response of damaging Philippines tropical cyclones to a warming climate using the pseudo global warming approach

It is advisable to refer to the publisher's version if you intend to cite from the work. See [Guidance on citing](#).

the End User Agreement.

www.reading.ac.uk/centaur

CentAUR

Central Archive at the University of Reading

Reading's research outputs online

Response of damaging Philippines tropical cyclones to a warming climate using the pseudo global warming approach

Rafaela Jane Delfino[1,2] · Pier Luigi Vidale[1] · Gerry Bagtasa[2] · Kevin Hodges[1]

Abstract

The potential changes in the characteristics and damage potential of three of the most damaging tropical cyclone (TC) events (Haiyan 2013, Bopha 2012, Mangkhut 2018) in the Philippines have been simulated using the pseudo global warming (PGW) technique. Simulations were performed using the Weather Research and Forecasting model at 5 km resolution with cumulus parameterization (5 kmCU) and 3 km without cumulus parameterization (3 kmNoCU), with PGW deltas derived from a selection of the CMIP6 models. We found that re-forecasting the three TCs under future warming leads to more intense TCs, with changes in maximum wind of 4%, 3%, and 14% for the 5 kmCU runs, and 14%, 4%, and 12% for the 3 kmNoCU runs of Typhoon Haiyan, Bopha, and Mangkhut, respectively. The changes in track, translation speed, and size are relatively small. The TC cases have a higher impact potential in the future, as expressed by the cyclone damage potential index, ranging from ~1% to up to 37% under the SSP5-8.5 scenario. Based on the pre-industrial runs, climate change has had, so far, only a weak influence on TC intensity and not much influence on track, translation speed, and size. Simulations without convective parameterization show similar changes in the sign of the projected TC intensity response, but different signals of change in translation speed and size.

1 Introduction

The Philippines has high exposure to tropical cyclones (TCs) which often result in casualties and significant damage to property due to strong winds and flooding from storm surges and associated rainfall. The effect of climate change on TC activity and its characteristics is of major interest and practical importance in the Philippines, given the socioeconomic consequences produced by TCs. Most studies predict a decrease in the frequency of TCs in the future, but an increase in the intensity (high confidence) and number of intense TCs (low confidence), and TC-associated rainfall globally (Walsh et al. 2019; Knutson et al. 2020; Knutson et al. 2021) as well as in the Western North Pacific (WNP) Basin (Christensen et al. 2013). There is still no clear consensus on TC translation speed projections (Knutson et al. 2020), which could lead to damage from accumulated and prolonged rainfall, as well as prolonged exposure to strong winds. In the Philippines, estimates are broadly consistent with global research results on TC activity, which predict a decrease in TC frequency in the future (Gallo et al. 2019), but an increase in the frequency of strong TCs (Walsh et al. 2016 and Sugi et al. 2017) and an increase in TC-related rainfall (Daron et al. 2016).

Global climate models (GCMs) are critical tools for projecting future changes and trends in extreme weather and climate events. However, owing to their typically coarse resolutions and model biases, GCMs have problems to replicate observed TC properties. This is despite considerable breakthroughs in the use of high-resolution GCMs (Roberts et al. 2020; Manganello et al. 2014; Murakami et al. 2012) and global convection-permitting models in modeling TCs in recent decades (Gutmann et al. 2018; Judt et al. 2021; Kendon et al. 2021; Yamada et al. 2017) However, GCMs

✉ Rafaela Jane Delfino
  r.p.delfino@pgr.reading.ac.uk; rpdelfino@up.edu.ph

1 Department of Meteorology, University of Reading, Reading, UK

2 Institute of Environmental Science and Meteorology, University of the Philippines - Diliman, Quezon City, Philippines

at high resolutions require very high to extensive computing resources. A useful alternative approach to increase the understanding of the changes in TC activity and their characteristics, for the purpose of simulating event-based, or seasonal to inter-annual variability and long-term climatological changes, is the use of downscaling. It encompasses both dynamical downscaling using Limited Area Models (LAMs) and statistical downscaling methods (Knutson et al. 2013; Xu et al. 2019; Chen et al. 2020; Emanuel et al. 2008, 2020). Statistical downscaling methods have been found to be good over the historical period since they are tuned with observations. However, the empirical relationships between large-scale predictors (e.g., GCM-derived atmospheric parameters) and local predictands (e.g., winds, rainfall) are assumed to also hold in the future (Camargo and Wing 2016) which may not be correct. Dynamical downscaling with LAMs, used as regional climate models for long-term seasonal or climate simulations or as numerical weather prediction for short-term weather forecasting, can realistically capture the processes relevant to the formation and evolution of TCs but are still dependent on parameterizations (Seneviratne et al. 2021; Gallo et al. 2019; Daron et al. 2018). However, it is important to note, that the performance of dynamical downscaling using LAMs is strongly affected by the quality of the boundary forcing data i.e., output from GCMs (Holland et al. 2010; Liu et al. 2019).

There are different approaches to understanding the climate change effects on TC characteristics at higher resolution using dynamic downscaling (e.g., Lynn et al. 2009; Lackmann 2015). Adachi and Tomita (2020) provide a summary of these different approaches including the Pseudo Global Warming (PGW) approach. Lynn et al. (2009) performed current and future simulations of Hurricane Katrina (2005) using the PGW method and found decreases in the minimum central pressure but also decreases in the mean and maximum wind speeds, maybe due to the shift in Katrina's simulated track. The PGW technique allows us to examine the change of characteristics of historical TC cases under future and even past climate conditions (Takayabu et al. 2015; Parker et al. 2018; Patricola and Wehner 2018; Chen et al. 2020). Lackmann (2015) used convection-permitting simulations to look at changes in Hurricane Sandy (2012) due to the mean changes in temperature and humidity in the future and found decreases in the minimum central pressure. Nakamura et al. (2016) used the same technique for Typhoon Haiyan and showed that Typhoon Haiyan became more intense if only the sea surface temperature (SST) is changed and less intense if SST, atmospheric temperature (ATM) and relative humidity (RH) are changed in the future conditions. Parker et al. (2018) conducted PGW simulations for three TCs that made landfall in Australia and found that the TC cases are more intense (reduced sea level pressure and increased wind speeds) and have more rainfall. Patricola

and Wehner (2018) also applied the same technique, but with higher resolution convection-permitting regional climate simulations for several TC case studies across the globe (including Typhoon Haiyan) and found that these TCs intensify in the future simulations and have greater rainfall amounts. Chen et al. (2020) looked at the potential future changes of three landfalling TCs in the Pearl River delta using the PGW technique and simulated the potential changes in storm surge activity. Their results showed increases in the peak intensities of the TCs and a corresponding increase in storm surge. Mittal et al. (2019) and Reddy et al. (2021) also conducted similar experiments on different TC cases in the Bay of Bengal. The former simulated Phailin (2013) and found a stronger and bigger storm in the future, with no change in translation speed. The latter looked at three TC cases and found increased winds and rainfall, reduction in translation speeds, and deepening of the TC core and higher damage potentials. Gutmann et al. (2018), on the other hand, performed a 13-year convection-permitting simulation of 22 TC cases in the Atlantic Ocean and found increased maximum winds, lower central pressure, slower translation speeds, and higher precipitation rates, with varying degrees and magnitude of responses across the 22 TC cases. With the differences in changes in TC characteristics shown in previous studies in different basins, it is important to look at the potential response of TC characteristics to climate change in the WNP basin, particularly in the Philippines.

In addition, the PGW technique has also been used to investigate whether present-day climate change has already affected TCs in the Atlantic Basin (Patricola and Wehner 2018) and in Japan (Kawase et al. 2021). Using simulations from a 4.5 km convection permitting Weather Research and Forecasting (WRF) model, Patricola and Wehner (2018) found that climate change has so far increased rainfall of Hurricanes Irma, Katrina, and Maria but did not influence their intensities. On the other hand, Kawase et al. (2021) found that historical warming has already increased the intensity of Typhoon Hagibis (2019), along with its associated precipitation over Japan. So far, there is no consensus regarding whether climate change has already influenced tropical cyclone frequency and intensity due to the large natural variability and long-term data heterogeneity. Studies such as that of Patricola and Wehner (2018) and Kawase et al. (2021) may help provide evidence as to whether climate change has already influenced TC activity. We provide additional evidence towards understanding the link between climate change and TCs, primarily looking at how climate change has so far affected TCs in the Philippines.

Previous studies that used the PGW technique highlighted the importance of looking at multiple TC cases (Nakamura et al. 2016; Parker et al. 2018; Gutmann et al. 2018; Mittal et al. 2019) with varying TC intensities

(Nakamura et al. 2016) in different seasons to identify outliers in TC response to future climate conditions (Parker et al. 2018). These past studies did not investigate the uncertainties associated with the use of different GCMs (Parker et al. 2018; Patricola and Wehner 2018; Mittal et al. 2019; Reddy et al. 2021) which is relevant in accounting for the uncertainty due to the potential range of sensitivities brought about by different models. The innovations in our study are: (1) investigating the different TC cases with observed varying intensity, landfall area, and months of occurrence; (2) the simulations were forced with initial and boundary conditions from several GCMs contributing to the Coupled Model Inter-comparison Project Phase 6 (CMIP6) (Eyring et al. 2016) and looking at different factors such as sea surface temperature, atmospheric temperature and relative humidity; (3) the WRF's simple mixed-ocean layer model was used in order to incorporate the atmosphere–ocean feedback during the passage of TCs; and (4) we tested the sensitivity to different cumulus schemes and initialization times. We have also attempted to identify the physical mechanisms driving the simulated TC responses and discuss relevant underlying uncertainties.

This study aims to analyze how the characteristics and potential impacts of the most damaging TC events in the Philippines might change under future climate conditions using dynamical downscaling with the high-resolution WRF, configured for the Southeast Asia region centered on the Philippines, as in Delfino et al. (2022a, b), and using the PGW technique. We aim to answer the following questions:

- How might the most damaging TC events in the Philippines i.e., Typhoons Haiyan (2013), Bopha (2012) and Mangkhut's (2018) respond to past (pre-industrial) and future climate change perturbations derived from the latest CMIP6 GCMs?
- How do the added PGW deltas (warming signals i.e., surface and atmospheric warming; with or without relative humidity) affect TC characteristics?
- How much of the uncertainty in the TC responses is caused by the convective parameterization?

The rest of this paper is organized as follows: Sect. 2 presents a brief description of the TC cases, experimental design and methodology; Sect. 3 describes the simulated changes in the large-scale atmospheric variables (Sect. 3.1), and changes in the TC characteristics (3.2), discussion of the physical mechanisms behind the changes in TC characteristics (3.3) and cyclone damage potential (3.3) Sect. 3.2 is further separated in two sub-sections presenting the results of the different forcings under future climate (3.2.1) and the changes due to the different resolutions under past and future climate (3.2.2) The summary and conclusions are presented in Sect. 4.

2 Data, experimental design, and methods

2.1 Data

The European Centre for Medium-Range Weather Forecasts (ECMWF) Re-analysis 5th Generation (ERA5) is used for both the initial and boundary conditions for the simulations under the current climate. The data is available from https://cds.climate.copernicus.eu/. It is the latest generation of reanalysis products produced by ECMWF with horizontal resolution of 31 km, hourly temporal resolution and 137 atmospheric levels (Hersbach et al. 2020). ERA5 utilizes the best available observational data from satellites and in-situ stations, which are quality controlled and assimilated using a state-of-the-art 4-dimensional data assimilation system (4D-VAR) (Isaksen et al. 2010) in and the ECMWF's Integrated Forecast System (IFS) Cycle 41r2.

The TC best-track information used here for verifying the simulations is taken from the World Meteorological Organization (WMO) subset of the IBTrACS (IBTrACS-WMO, v03r09) which was taken from the best-track data provided by the Japan Meteorological Agency (JMA). The CMIP6 GCM data were downloaded from https://www.esgf-index1.ceda.ac.uk/search/cmip6-ceda/.

We used data from CMIP6 models for the far-future period of 2070–2099 and the worst-case/high-emission scenario from the suite of Shared Socio-economic Pathways (SSP) 5–8.5. The pre-industrial run covers the period between 1850 and 1899 and the current climate covers the period between 1970 and 2000. Under the pre-industrial climate, the PGW delta was calculated by adjusting the same variables from the historical 1970–2000 monthly mean minus the pre-industrial 1850–1899 monthly mean, then added to the current ERA5 initial and boundary condition. Four CMIP6 models were selected based on a subset of the CMIP6 GCMs (see Supplementary Fig. 1) analysed in Emanuel (2020) and that correspond to a range of Transient Climate Response (TCR) and Equilibrium Climate Sensitivity (ECS) (Meehl et al. 2020) which are expected to provide a good range of potential storylines for the TC cases (Vecchi et al. 2019). The TCR and ECS were used as proxies, to make sure that our simulations would experience a wide range of warming levels and of changes in environmental conditions. We have used these proxies, therefore, to provide a representative and relevant set of storylines considering the following: (a) small to large changes in magnitude of global warming; (b) magnitude of SST change in the region; and (c) patterns of SST change

Table 1 CMIP6 model names, Equilibrium Climate Sensitivity (ECS), Transient Climate Response (TCR), resolution, sources, institution, and references of the GCMs used in this study

CMIP6 model name	ECS (°C)	TCR (°C)	Horizontal resolution	Institution	Reference
HadGEM3-C31-LL	5.6	2.6	1.25°×1.88°	United Kingdom Met Office Hadley Center	Sellar et al. (2020)
CESM2	5.2	2.0	1.25°×0.93°	National Center for Atmospheric Research	Danabasoglu et al. (2020)
MIROC6	2.6	1.6	1.4°×1.4°	Center for Climate System Research, University of Tokyo, JAMEST, NIES	Tatebe et al. (2019)
MPI-ESM1-2-HR	3.0	1.7	0.94°×0.94°	Max Planck Institute	Mulller et al. (2018)

Sources: https://www.science.org/doi/10.1126/sciadv.aba1981#T2 and https://www.wcrp-cmip.github.io/CMIP6_CVs/docs/CMIP6_source_id.html

in the region. The description of the selected models is presented in Table 1.

2.2 TC case studies

For this study, we have chosen the three of the most damaging TCs to have affected the Philippines between 1970 to 2020 (Lara 2020) – Typhoon Haiyan (2013), Typhoon Bopha (2012), and Typhoon Mangkhut (2018). Typhoons Haiyan and Bopha are also in the top five deadliest TCs in recorded history in the Philippines. These TC cases were also selected to represent the three main regions of landfall– Luzon for Mangkhut, Visayas for Haiyan, and Mindanao for Bopha. Table 2 provides a brief description of the three TC cases, arranged according to the estimated cost of damages. For more details of the TC Cases, see Delfino et al. (2022b).

2.3 Experimental design and model setup

The three TCs were simulated using the Advanced Research Weather Research and Forecasting (WRF-ARW) model version 3.8.1 (Skamarock et al. 2008). The WRF model has been used extensively in simulating TCs in the Philippines (Flores 2019; Aragon and Pura 2016; Spencer et al. 2012; Islam et al. 2015; Lee and Wu 2018; Cruz and Narisma 2016). The model setup and configurations,

based on previous sensitivity experiments (see Delfino et al. 2022a, b; Bagtasa 2021), are detailed in Table 3. Data from ERA5 was used as initial and boundary conditions for the control simulations and the augmented initial and boundary conditions obtained from adding the PGW deltas were used for the future simulations. By comparing these future simulations with the control runs, we can therefore infer the responses of the TC cases to future climate conditions. Simulations under the current and future climate (with surface and air temperature, and relative humidity deltas) were performed with four different initialization times (with 6-hourly intervals) to construct ensemble members, performed using a two-way nest of 25 km and 5 km outer and inner domain, respectively, where the cumulus parameterization is turned on in both outer and inner domains. This experimental configuration is referred to as 5 kmCU (Table 4). Two-way nesting configuration has been used in previous TC case studies in the Philippines (e.g., Delfino et al. (2022a); Mori et al. (2014), Takayabu et al. (2015), Nakamura et al. (2016) and other PGW studies in other TC basins (Parker et al. 2018; Davis et al. 2008; Mittal et al. 2019; Reddy et al. 2021). We also performed simulations at a convection-permitting horizontal resolution of 3 km where the cumulus parameterization is turned off in the 3 km inner domain, referred to as 3 kmNoCU, to account for the uncertainty in the use of cumulus parameterization

Table 2 Description of the three TC case studies

TC case study international (local) name and year	Observed minimum central pressure (hPa)	Landfall Region (latitude of formation)	Outer domain maximum SST from ERA5 at initialization (global mean observed monthly SST anomaly* & ENSO conditions**)	Cost of damage***
Haiyan (Yolanda) 2013	895 hPa	Visayas (5.8°N)	30.5 °C (0.58, Neutral)	₱95.5 B/$2.2B
Bopha (Pablo) 2012	930 hPa	Mindanao (3.4°N)	28 °C (0.47, mod LN)	₱43.2B/$1.06B
Mangkhut (Ompong) 2018	905 hPa	Northern Luzon (11.8°N)	30.6 °C (0.69, weak EN)	₱33.9B/$627 M

Legend: *global mean observed monthly SST anomaly (Source: NOAA 2021); ** ENSO El Nino Southern Oscillation conditions (LN: La Nina; EN: El Nino) (Source: CPC, 2018, 2021) and *** estimated cost of damage in agriculture and infrastructure (Source: NDRRMC 2012, 2014, 2018)

Table 3 Model setup and physics parameterization

Experiment	5 kmCU	3 kmNoCU
Number of Domain	Two (outer coarse domain D01 & inner domain D02)	One (D01)
Nesting	Two-way (between D01 & D02)	None
Grid resolutions	25 km (D01); 5 km (D02)	3 km (D01)
Grid spacing	295×160 (D01), 746×551 (D02)	895×660 (D01)
Number of vertical eta levels	44 (D01), 44 (D02)	44 (D01)
Cumulus parameterization	Kain–Fritsch scheme (Kain 2004) – D01 & D02	None (D01)
Cloud microphysics	WRF Single–moment 6–class Scheme for the cloud microphysics (Hong and Lim 2006) – D01 & D02 (5 kmCU); D01 (3 kmNoCU)	
Longwave radiation	RRTM scheme (Rapid Radiative Transfer Model) (Mlawer et al. 1997)	
Shortwave radiation	Dudhia scheme (Dudhia 1989) – D01 & D02 (5 kmCU); D01 (3 kmNoCU)	
Surface layer	MM5 Monin–Obukov scheme (Monin and Obukhov 1954) – D01 & D02 (5 kmCU); D01 (3 kmNoCU)	
Land surface scheme	Unified Noah Land Surface Model (Chen and Dudhia 2001; Tewari et al. 2004) – D01 & D02 (5 kmCU); D01 (3 kmNoCU)	
Planetary boundary layer scheme	Yonsei University (YSU) PBL scheme (Hong et al. 2006) – D01 & D02 (5 kmCU); D01 (3 kmNoCU)	
Surface flux option	isftcflx = 1	
Atmosphere–ocean feedback	1D Ocean Mixed Layer Lapse rate: 0.14 °C m^{-1} Mixed Layer Depth: 50 m	

Table 4 Summary of experiments with different forcings and GCMs

Simulation Group/Code	Variables with PGW Delta*	GCM PGW delta forcing	Period	Experiment	Case Study (Initial Times)
Control (CTRL)	None	None	Current	5 kmCU	Haiyan (04 Nov 00UTC) Bopha (02 Dec 00UTC) Mangkhut (10 Sep 00UTC)
Surface (SFC) / SFC-only	Surface (land and sea) temperature	CESM2	Current Future	5 kmCU	Haiyan (04 Nov 00UTC) Bopha (02 Dec 00UTC) Mangkhut (10 Sep 00UTC)
		HadGEM3	Current Future	5 kmCU	
SFC + Pressure Level (PLEV)	Surface (land and sea) temperature, air temperature	CESM2	Current Future	5 kmCU	Haiyan (04 Nov 00UTC) Bopha (02 Dec 00UTC) Mangkhut (10 Sep 00UTC)
		HadGEM3	Current Future	5 kmCU	
		MPI	Current Future	5 kmCU	
		MIROC6	Current Future	5 kmCU	
FULL	Surface (land and sea) temperature, air temperature, relative humidity	CESM2	Current Future	5 kmCU	Haiyan (04 Nov 00UTC) Bopha (02 Dec 00UTC) Mangkhut (10 Sep 00UTC)
		HadGEM3	Current Future	5 kmCU	
		MPI	Current Future	5 kmCU	
		MIROC6	Current Future	5 kmCU	

*All experiments also include pressure (surface and sea level) and geopotential height PGW deltas

as studies have shown that convection-permitting models improve the simulation of TCs (Li et al. 2018; Gutmann et al. 2018). To evaluate the effect of climate change until the present time, we performed experiments representing Typhoons Haiyan, Bopha, and Mangkhut as if they were to occur in a pre-industrial climate with four different initial times for both 5 kmCU and 3 kmNoCU experiments

Table 5 Summary of experiments on the different resolutions and different periods (pre-industrial and future)

Simulation group/code	Variables with PGW Delta	GCM delta forcing	Period	Initial Times
5 km CU	Surface and air temperature, pressure, geopotential height, relative humidity	CESM2	Pre-industrial Current Future	Haiyan (04 Nov 00UTC, 06UTC, 12UTC, 18UTC); Bopha (02 Dec 00UTC, 06UTC, 12UTC, 18UTC); Mangkhut (10 Sep 00UTC, 06UTC, 12UTC, 18UTC)
3 kmNoCU	Surface and air temperature, pressure, geopotential height, relative humidity	CESM2	Pre-industrial Current Future	Haiyan (04 Nov 00UTC, 06UTC, 12UTC, 18UTC); Bopha (02 Dec 00UTC, 06UTC, 12UTC, 18UTC); Mangkhut (10 Sep 00UTC, 06UTC, 12UTC, 18UTC)

(Table 5). The summary of the PGW experiments is presented in Tables 4 and 5.

2.4 Pseudo-global warming (PGW) technique

This study used the PGW method introduced by Schär et al. (1996) as a surrogate climate change method and later used in various studies (Kimura and Kitoh 2007; Sato et al. 2007; Knutson et al. 2008; Nayak and Takemi 2020). The PGW technique adds a climate perturbation signal to the present-day conditions for the period of interest. The initial and boundary conditions are generated by combining 6-hourly reanalysis data (ERA-5) and climatological monthly mean perturbations that are extracted from the GCMs. The result is the forcing data for the alternative climate, called the PGW condition or climate change delta. It can then be used as the WRF initial and boundary conditions for climate simulations of the TC case studies. The PGW technique is one method of evaluating the impacts of different climate change scenarios such as global warming on past TCs. Other methods are presented in Adachi and Tomita (2020), a summary of which is presented in Supplementary Table 1, and a new approach is being proposed by Dai et al. (2020) to combine the transient weather signal from one GCM simulation with the monthly mean climate states from multi-GCM ensemble mean for the periods of interest. In most studies, the downscaled PGW condition is compared to the historical or present/current-day condition developed from reanalysis data to determine the projected change in the future climate for example. It is also well-suited for a storyline approach, which investigates the impact on an event intensity, as compared to the risk-based approach which investigates the impact on an event frequency (Shepherd et al. 2018).

The PGW delta was calculated by subtracting the monthly means (i.e., November for Haiyan, December for Bopha, and September for Mangkhut) of the current simulations from the future climate projected by each of the GCMs. The calculated PGW deltas for each variable were then added to the 6-hourly ERA-5 initial and boundary conditions for the three TC cases to build the PGW conditions. The PGW delta was calculated in the initial and lateral boundary conditions for the following variables: surface (land and sea) and air temperature, pressure (surface and sea level), geopotential height and relative humidity (RH), as used in previous PGW studies (Patricola and Wehner 2018, Parker et al. 2018). There is disagreement in the literature regarding whether the RH should be allowed to change in future simulations. Some PGW studies (e.g., Parker et al. 2018; Mittal et al.2019; Chen et al. 2020; Reddy et al. 2020; Lackmann et al. 2015) have applied a delta to the RH, but there are also examples where RH is not changed (e.g., Kawase et al. 2009; Patricola and Wehner 2018) where it is argued that: (1) an inconsistency is created when adding a broadly uniform,

GCM-derived specific humidity delta onto a specific synoptic pattern and (2) RH is generally expected to remain constant in the future. Based on the results of Parker et al. (2018), the inclusion or exclusion of the RH delta does not affect the overall results. For this study, we have decided to experiment with changes in RH, in order to further understand its effects on TC response (FULL experiments).

2.5 TC tracking method

The simulated track and intensity values were obtained every 6 h using the TRACK algorithm (Hodges et al. 2017) as used in Hodges and Klingaman (2019). TRACK determines TCs as follows: first the average of the relative vorticity at 850-, 700-, and 600-hPa levels is obtained and averaged. The field is then spatially filtered using 2D discrete cosine transforms equivalent to T63 spectral resolution and the large-scale background is removed. The feature points are determined by first finding the grid point relative vorticity maxima $> 5.0 \times 10^{-6}$ s^{-1} which are then used as starting points for a B-spline interpolation and steepest ascent maximization method to determine the off-grid feature points (Hodges 1995 as cited by Hodges and Klingaman 2019) that results in smoother tracks. The tracking is performed by first initializing the feature points into tracks using a nearest neighbour method and then refining them by minimizing a cost function for track smoothness subject to adaptive constraints (Villafuerte et al. 2021). The tracking is done for the entire simulation period. After completing the tracking, other variables are added to the tracks, including the maximum 10-m winds and minimum central pressure at full resolution. This is done by searching for the maximum 10-m winds within a 6° geodesic radius, and for the true minimum mean sea level pressure within a 5°-radius using the B-splines and minimization method (Hodges and Klingaman 2019). In addition, the TC vertical structure or profile was also taken using the TRACK algorithm by calculating the tangential, and radial winds at peak intensity at height levels between 0 and 18 km on a radial grid with geodesic radius of 10° (Bengtsson et al. 2007) for each simulation.

2.6 Cyclone damage potential

The potential damage that can be caused by the TCs is calculated using the cyclone damage potential (CDP) index (Done et al. 2018; Holland et al. 2016), formulated using critical cyclone parameters that involve the maximum wind (or energy dissipated at the surface), size (radial extent) and translation speed, and is given by:

$$CDP = \frac{4\left[\left(\frac{Vmax}{65}\right)^3 + 5\left(\frac{HFWrad}{50}\right)\right]}{TS} \tag{1}$$

where Vmax and TS are the maximum surface wind speed and translation speed, respectively, both expressed in ms^{-1}. Vmax here is the maximum of 10 m wind speed over the inner domain. The translation speed of the TC for the current time step is calculated as a centered difference. The radius of the hurricane winds (HFWrad) is calculated by determining the radial distance between the storm center and the outermost point from the storm center where the wind speed is equal to 33 ms^{-1}. The CDP index is computed only if Vmax is greater than 33 ms^{-1}. If TS < 2.6 ms^{-1}, then TS is set to be as 2.6 ms^{-1}. The CDP index value ranges from 0 to 10. A higher CDP indicates an increased risk of TC-related damage costs, particularly damage brought about by wind (Holland et al. 2016).

3 Results and discussion

3.1 Large-scale conditions under future and pre-industrial climate

Based on the future climate change signals calculated from these four GCMs, the mean SST change in the experiment domain for the far future is projected to be between 1.89 °C to 3.65 °C warmer, with SST increases ranging between 2.16 °C to 3.27 °C in November; 2.13 °C to 3.12 °C in December; and 1.89 °C to 3.65 °C in September under the SSP5-8.5 scenario (Fig. 1). Figure 1a, 1b and 1c shows the increases in SST from the CESM2 model for November, December, and September with mean SST changes of 3.22 °C, 3.09 °C and 2.94 °C, respectively. The most substantial increases in SST are found from HadGEM3 (Fig. 2d–f and least increases are found from the MIROC (Fig. 1g–i) and MPI (Fig. 1j–l) models. The vertical distribution of air temperature is also shown on Fig. 2a–c for November, December, and September, respectively, which shows that the air temperature will be ∼ 3–6 °C warmer on the average, with stronger warming in the upper level (near 250 hPa), leading to the atmosphere being more stable in the future under SSP5-8.5 (Fig. 2). This bulge of warming in the upper troposphere is consistent with previous studies (Hill and Lackmann 2011; Knutson and Tuleya 2004). The RH in the troposphere, particularly in the mid-troposphere, shows minimal change in the future climate under the SSP5-8.5 scenario (Fig. 2d–f).
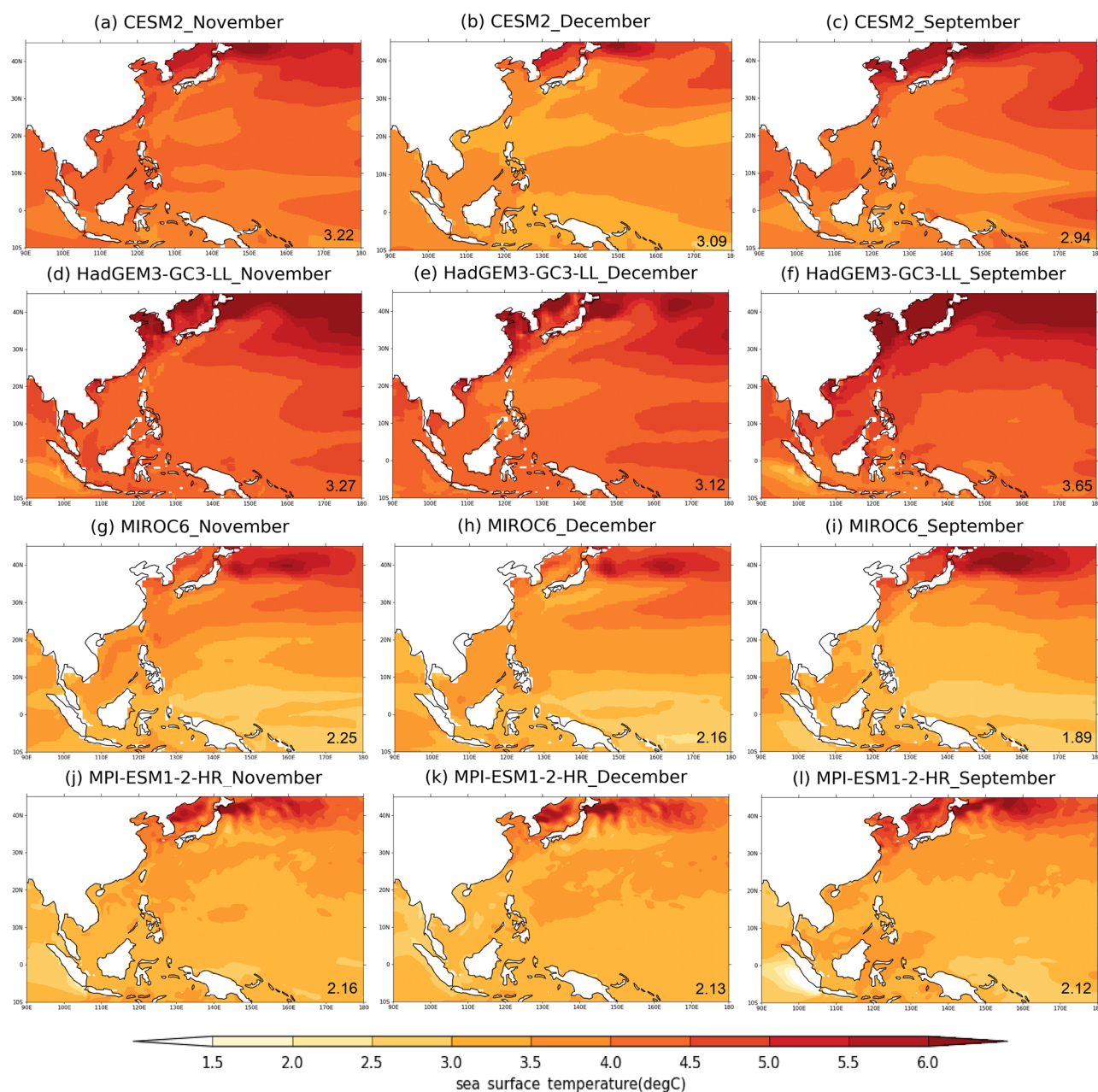
Fig. 1 The November (left panels), December (middle panels) and September (right panels) monthly mean sea surface temperature delta (°C) added to the boundary and initial conditions of the control runs for Typhoons Haiyan, Bopha, and Mangkhut, respectively, to create the future clim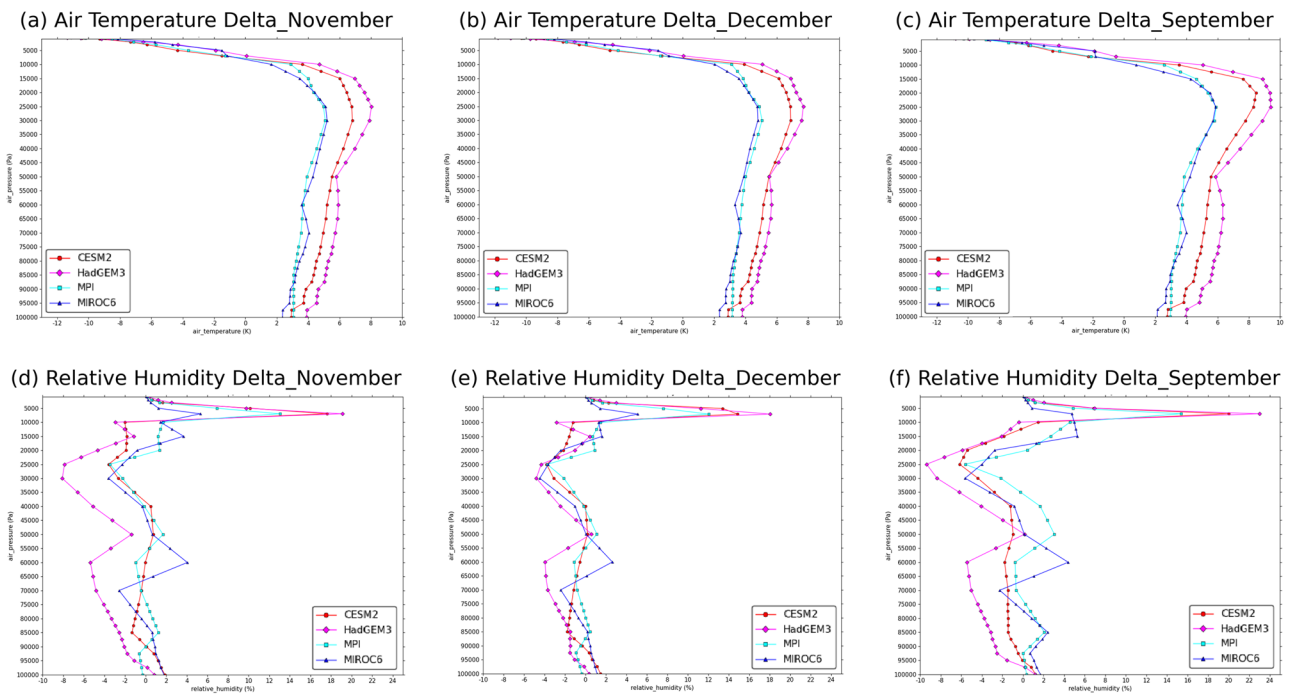ate scenario change in far future (2070–2099) from CMIP6 models (CESM2-**a–c**; HadGEM3-**d–f**; MIROC6-**g–i**; and MPI-**j–l**) according to the SSP5-8.5 scenario relative to the historical period (1970–1999). The domain-averaged delta SSTs are indicated in the lower right hand corner

In the pre-industrial climate, the change in SST ranges between − 0.03 to more than − 0.2 °C (see Supplementary Fig. 2), the changes in SST and the change in air temperature and relative humidity are also shown in Supplementary Fig. 3.

3.2 Changes in TC characteristics

3.2.1 Changes due to different forcings and GCMs

Nakamura et al. (2016) showed that atmospheric and surface temperature warming has opposing influence on Haiyan's intensity under future climate conditions. The results of the experiments with different forcing and GCMs are

Fig. 2 The November (left panels), December (middle panels) and September (right panels) monthly mean air temperature delta (°C) (top panels) and relative humidity delta (%) (bottom panels) added to the boundary and initial conditions of the control runs for Typhoons Haiyan, Bopha, and Mangkhut, respectively, to create the future climate scenario change in far future (2070–2099) from CMIP6 models (CESM2, HadGEM3, MIROC6 and MPI) according to the SSP5-8.5 scenario relative to the historical period (1970–1999)
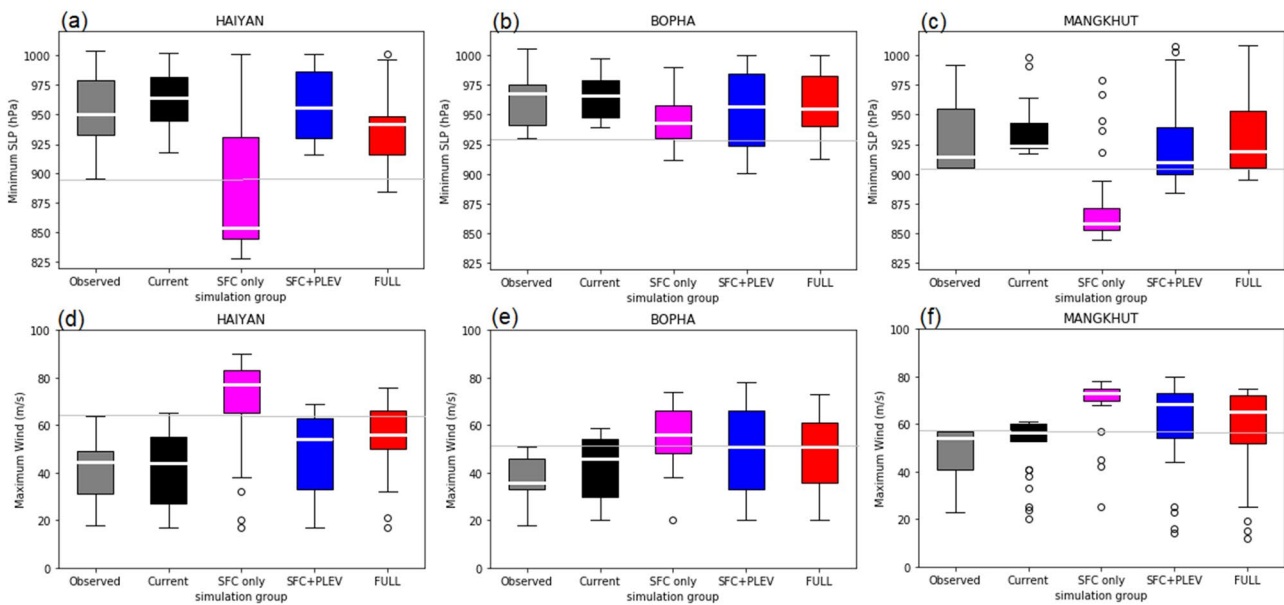
Fig. 3 Boxplots of the minimum central pressure in hPa (upper panels, **a**–**c**) and maximum 10-m wind speed in ms^{-1} (lower panels, **d**–**f**) throughout the lifetime of the different TC cases from current climate simulations (black) and the mean of the future climate simulations (SSP5-8.5 scenario) with the surface only (SFC) experiments (magenta, sfc), surface and atmospheric level (SFC+PLEV) experiments (blue) and surface and atmospheric level with relative humidity (FULL) experiments (red); of the different TC case studies—(**a**, **d**) Haiyan (left), (**b**, **e**) Bopha (center) and (**c**, **f**) Mangkhut (right). Center white line denotes the median, box limits denote lower and upper quantiles, whiskers denote maximum and minimum, and the circles denote the outliers. Solid gray horizontal lines are the observed minimum central pressure (maximum winds) 895 hPa (64 ms^{-1}), 930 hPa (51 ms^{-1}), and 905 hPA (56 ms^{-1}) for Typhoon Haiyan, Bopha and Mangkhut, respectively

Table 6 Summary of changes in minimum central pressure (in hPa) and maximum 10-m wind speed (in ms^{-1}) between the future minus the current climate simulations

Simulation Group/Code	GCMs PGW delta forcings	Haiyan			Bopha			Mangkhut		
		Difference in Minimum central pressure (hPa)	Difference in Max Wind (ms^{-1})	Percent Change in Max Wind per °C change in SST	Difference in Minimum central pressure (hPa)	Difference in Max Wind (ms^{-1})	Percent Change in Max Wind per °C change in SST	Difference in Minimum central pressure (hPa)	Difference in Max Wind (ms^{-1})	Percent Change in Max Wind per °C change in SST
SFC-only	CESM2	−71	16	5	9	12	4	−61	17	6
	HadGEM3	−76	17	5	−22	15	5	−71	22	6
	Mean	**−73**	**16**	**5**	**−6.5**	**13**	**4**	**−66**	**19**	**6**
SFC+PLEV	CESM2	−2	4	1	−1	9	3	−13	11	4
	HadGEM3	−1	5	1	−1	9	3	−33	19	6
	MPI	−1	4	2	−6	8	4	−11	9	5
	MIROC6	−6	2	1	−11	8	4	−10	8	4
	Mean	**−3**	**4**	**1**	**−6.25**	**8**	**3**	**−16.75**	**12**	**5**
FULL	CESM2	−16	7	2	−5	9	3	−13	10	3
	HadGEM3	−27	7	2	0	7	2	−9	10	3
	MPI	−13	8	4	−4	8	4	−12	10	4
	MIROC6	−6	4	2	−1	9	4	−22	14	7
	Mean	**−15**	**6**	**2**	**−2.5**	**8**	**3**	**−14**	**11**	**4**
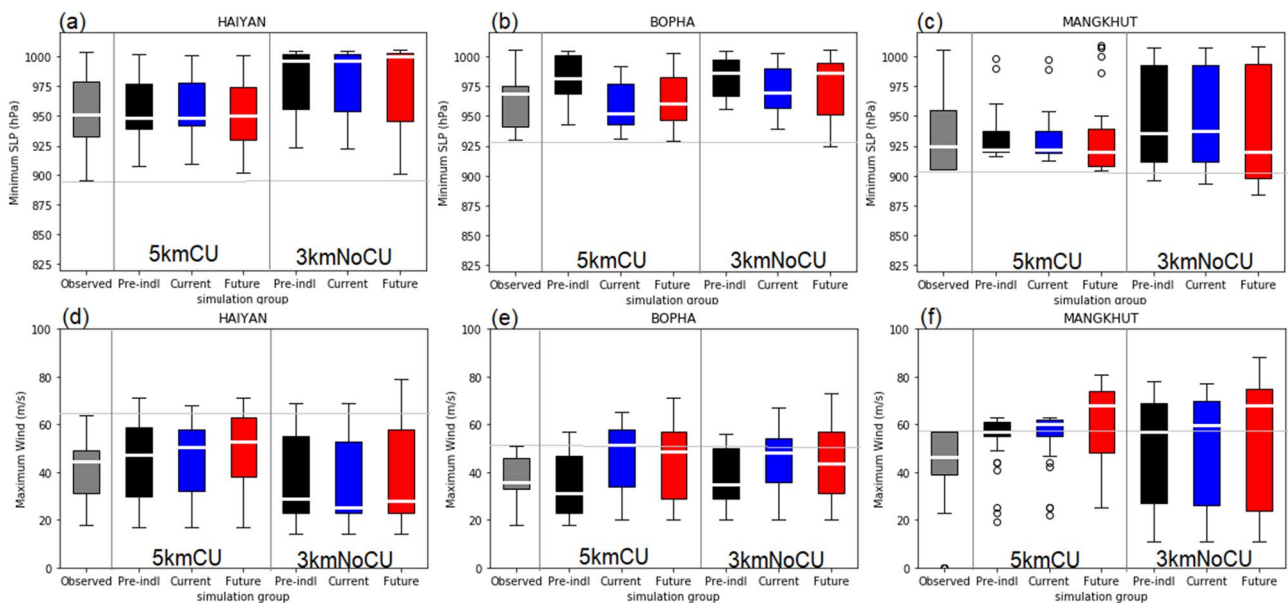
Fig. 4 Boxplots of the minimum central pressure in hPa (upper panels, **a**–**c**) and maximum 10-m wind speed in ms⁻¹ (lower panels, **d**–**f**) with the 5 kmCU vs 3 kmNoCU simulations throughout the lifetime of the different TC cases from current climate simulations (black) and the mean of the future climate simulations (SSP5-8.5 scenario) with the observed from IbTrACS (grey), simulations 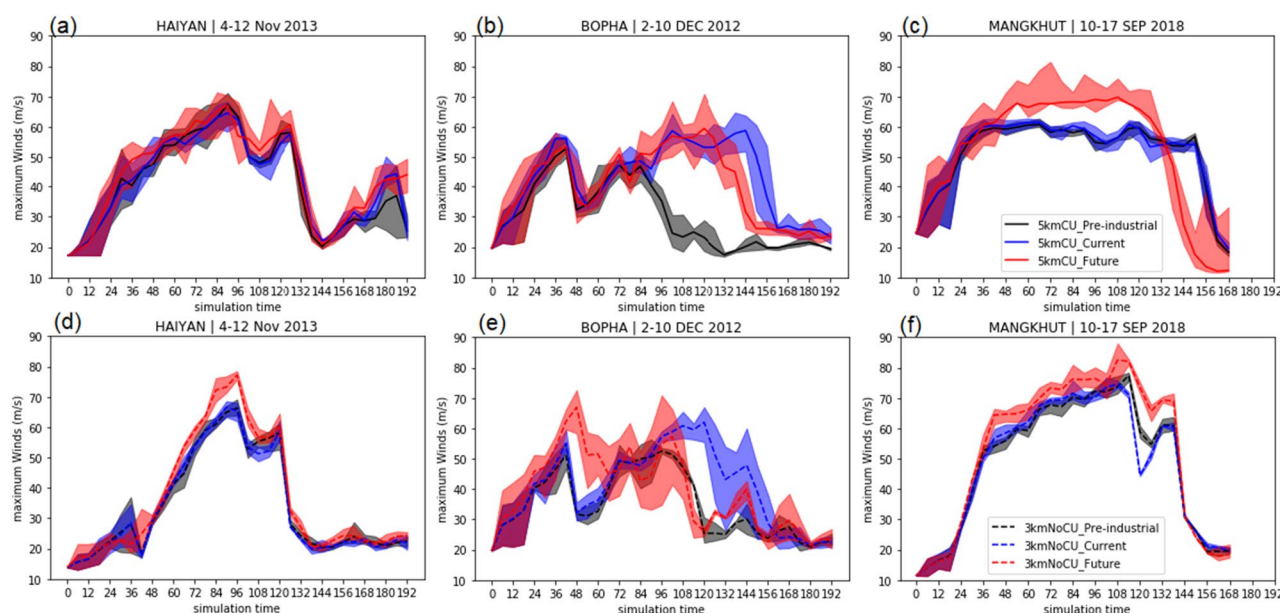under pre-industrial (black), current (blue) and future (red) climate of the different TC case studies—(**a**, **d**) Haiyan (left), (**b**, **e**) Bopha (center) and (**c**, **f**) Mangkhut (right). Center white line denotes the median, box limits denote lower and upper quantiles, whiskers denote maximum and minimum, and the circles denote the outliers. Solid gray horizontal lines are the observed minimum central pressure (maximum winds) 895 hPa (64 ms⁻¹), 930 hPa (51 ms⁻¹), and 905 hPA (56 ms⁻¹) for Typhoon Haiyan, Bopha and Mangkhut, respectively
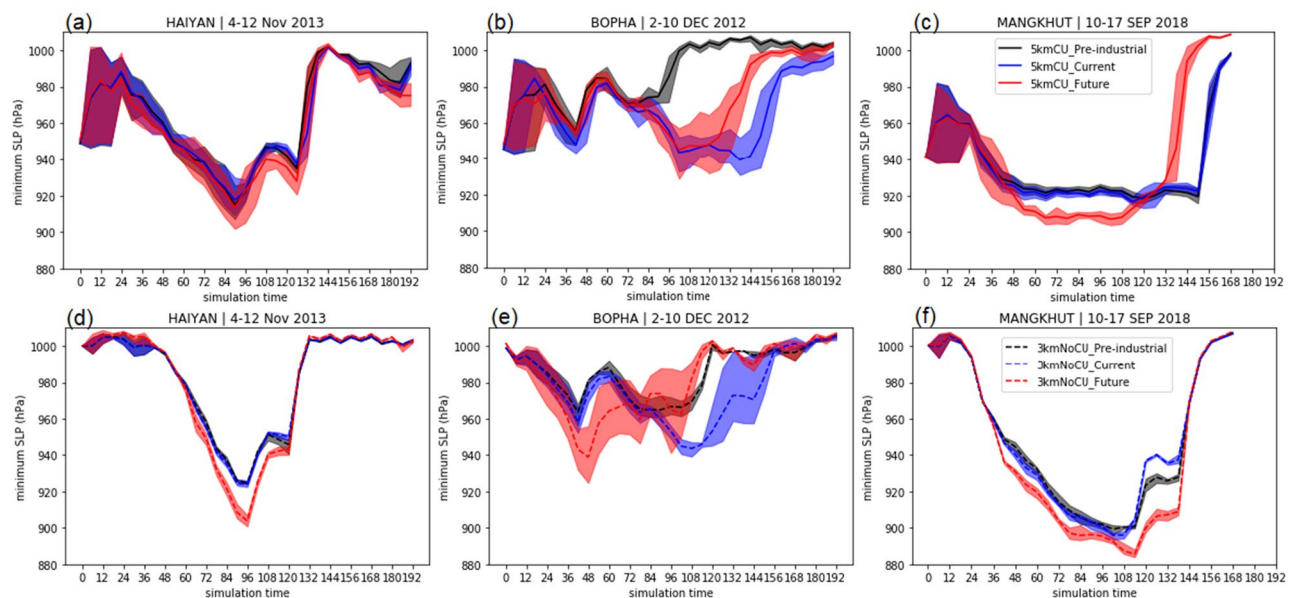
Fig. 5 Ensemble spread of the time series of the minimum central pressure (hPa) simulated from the 5 kmCU (top panels) and 3 kmNoCU (bottom panels) experiments under pre-industrial (black), current (blue) and future (red) climate for the different TC case studies—(**a**, **d**) Haiyan (left), (**b**, **e**) Bopha (center) and (**c**, **f**) Mangkhut (right). Solid and dashed lines denote the mean, and the spread denotes the simulated intensity from the four ensemble members initialized at different times

Fig. 6 Ensemble spread of the time series of the maximum winds simulated from the 5 kmCU (top panels) and 3 kmNoCU (bottom panels) experiments under pre-industrial (black), current (blue) and future (red) climate for the different TC case studies—(**a**, **d**) Haiyan (left), (**b**, **e**) Bopha (center) and (**c**, **f**) Mangkhut (right). Solid and dashed lines denote the mean, and the spread denotes the simulated intensity from the four ensemble members initialized at different times

summarized in Table 6. The SFC-only experiments show the greatest increase in intensity with reductions in minimum central pressure (and maximum winds) of up to − 73 hPa (16 ms^{-1}) for Haiyan, − 6.5 hPa (13 ms^{-1}) for Bopha and − 66 hPa (19 ms^{-1}) for Mangkhut. The TCs become more intense in the SFC + PLEV experiments with changes in atmospheric temperature, but not as intense as the SFC-only experiments, with mean changes in minimum central pressure (maximum winds) of − 3 hPa (4 ms^{-1}) for Haiyan, − 6.25 hPa (8 ms^{-1}) for Bopha and − 16.75 hPa (12 ms^{-1}) for Mangkhut. There is no significant difference when a humidity delta (FULL experiments) is added in the SFC + PLEV experiments with p-values of 0.1777 for Haiyan, 0.6745 for Bopha and 0.7671 for Mangkhut. The percent change in maximum wind per °C change in mean SST from the different of the GCM delta forcings under the FULL experiments are 2% for Haiyan, 3% for Bopha, and 4% for Mangkhut. This is within the projected TC maximum wind speeds increase of 5% (+1% to +10%) if the climate warms by 2 °C based on Knutson et al. (2021).

Overall, there is a range in the magnitude of changes due to the different GCM forcings which highlights the uncertainties associated with the use of different GCMs. However, the changes in intensity in the simulations forced by higher SST deltas (CESM2 and HadGEM3) and lower SST deltas (MPI and MIROC6) do not show systematic differences e.g., the simulations forced by HadGEM3 which has the highest

SST delta (mean of 3.27, 3.12 and 3.65°C for Haiyan, Bopha and Mangkhut, respectively) resulted in differences in maximum wind speed of 7 ms^{-1}, 7 ms^{-1}, and 10 ms^{-1} for Haiyan, Bopha and Mangkut, respectively under the FULL experiments. The simulations forced with MIROC6 which has a relatively lower SST delta (mean of 2.16, 2.13 and 2.12°C for Haiyan, Bopha and Mangkhut, respectively) resulted in differences in maximum wind speed of 4 ms^{-1}, 9 ms^{-1}, and 14 ms^{-1} for Haiyan, Bopha and Mangkut, respectively, also under the FULL experiments.

The boxplots in Fig. 3 show that there is a systematic shift towards higher intensities in the lifetime maximum intensity over the simulated lifecycle of the storms under future climate conditions for all experiments, with a reduction in central pressure and increase in the maximum winds, which are most apparent in the more intense Mangkhut and Haiyan, and not so much for Bopha. The minimum central pressure (maximum surface winds) reached 890 hPa (73 ms^{-1}) for Haiyan under the future climate (FULL) compared to 918 hPa (65 ms^{-1}) in the current climate. Mangkhut reached up to more than 70 ms^{-1} in the future climate (FULL) runs compared to 917 hPa (61 ms^{-1}) in the control.

To evaluate the response of the TC cases to climate change, the simulated TC tracks under current climate were first verified with observed TC tracks from the IBTrACS (Knapp et al. 2010) dataset. Indeed, the simulated tracks do not deviate substantially from the observed tracks under the

current, SFC + PLEV and FULL experiments. The surface warming only (SFC) experiments resulted in some differences in the simulated tracks (Supplementary Fig. 4), with the future climate simulations having a general tendency for the TCs to track more northwards than in the current climate (Bopha) and to recurve north and not make landfall in any part of the Philippines (Haiyan and Mangkhut). Despite some small deviations, the TC tracks under the future climate simulations are still within 3° away from the current climate simulation, a threshold that was found acceptable for this kind of analysis by Patricola and Wehner (2018).

We also looked at different parameters of TC size, which is defined here as the radius of different wind thresholds as used in Radu et al. (2014) i.e., gale-force winds (GFW, 17.5 ms^{-1}), damaging-force winds (DFW, 25.7 ms^{-1}), and typhoon- (or hurricane-) force winds (TFW, 33 ms^{-1}). The SFC-only experiments present an increase of up to 112% in the radius of maximum winds (RMW) and 60% in TFW. While the changes in size under the SFC + PLEV and FULL experiments are relatively small, with changes ranging from -7% up to 12% for all three TC cases.

3.2.2 Changes due to different resolutions in different periods

To investigate the uncertainty in the response of the TCs to climate forcings caused by convective parameterization, which was found to be the source of uncertainty in the current simulations of the TC cases (Delfino et al. 2022a), additional simulations of the three TC cases at a convection-permitting horizontal resolution of 3 km (3 kmNoCU) were performed. In addition, the three TC cases were also simulated under the pre-industrial climate to provide evidence as to whether CC has already influenced the TC characteristics.

We have found that the simulations using the 3 kmNoCU have almost the same response to that of the 5 kmCU simulations i.e., the TCs have relatively lower minimum central pressure and higher maximum surface winds in the future under the SSP5-8.5 scenario over the lifetime of the TCs (Fig. 4), and all throughout the simulation period (Figs. 5 and 6). The future response in minimum central pressure ranges from – 0.46%, – 0.07%, and – 1.20% for the 5 kmCU, and – 0.07%, – 0.43%, and – 1.11% for the 3 kmNoCU for Typhoon Haiyan, Bopha and Mangkhut, respectively. The mean (spread) percent change in maximum surface wind ranges between 4.09% (0 to 7%), – 2.68% (– 7 to 2%), and 15.57% (13 to 20%) for the 5 kmCU runs, and 13.75%, 4.28%, and 11.62% for the 3 kmNoCU runs of Typhoon Haiyan, Bopha and Mangkhut, respectively.

There are also relatively bigger spreads in the lifetime intensity of the TCs in the 3 kmNoCU compared to the 5 kmCU runs. This might be due to the relatively lower intensity at the start of the simulations (first 24 h) in the 3 kmNoCU runs compared to the 5 kmCU run (Fig. 5). During the TC's lifetime, the 3 kmNoCU runs achieve a deeper and more intense state. Figure 4 shows that the minimum of the central pressure is relatively lower in the 3 kmNoCU runs, and the maximum of the wind speeds is higher than in the 5 kmCU runs. The spread in the boxplots is largely due to the lower intensities in the 3 kmNoCU runs at the start and end of the simulations.

Of all the simulations, the 3 kmNoCU runs under future climate shows significant increases in intensity (at 1% and 5% level) for all three cases with p-value of 0.0003 and 3.712e-05 for Haiyan's minimum central pressure and maximum winds, p-value of 0.0317 and 0.0003 for Bopha's minimum central and maximum surface winds, and p-value of 0.0290 and 0.0738 for Mangkhut's minimum central and maximum surface winds. Haiyan (at 10% level) and Mangkhut (at 1% level) also showed significant intensity increases under the future climate in the 5 kmCU runs (Table 7).

For the three TC cases, the ensemble of the minimum central pressure and maximum surface winds are almost similar (Figs. 4, 5) under the current and pre-industrial climate conditions in both 5 kmCU and 3 kmNoCU runs, particularly for Typhoon Haiyan and Mangkhut, with some deviations after landfall for Bopha. However, in terms of peak intensity, in the more intense TCs Haiyan and Mangkhut, CC may have already had a weak influence on intensity in terms of relatively weaker winds than in the current climate (Fig. 3). In particular, the difference between the current and pre-industrial climate for minimum SLP (maximum wind) are 10 hPa (– 4 ms^{-1}) and – 9 hPa (4 ms^{-1}) for Haiyan and Bopha, respectively, while no mean difference for Mangkhut. For the 3 kmNoCU runs, Haiyan has a – 1 hPa (2 ms^{-1}), Bopha has – 19 hPa (10 ms^{-1})—significant at 1% level, and Mangkhut – 3 hPa (2 ms^{-1}) -significant at 5% and 10% respectively, current-pre-industrial difference (Table 7), which indicates that the TCs are relatively weaker under the pre-industrial climate than under the current climate simulations.

Figures 7 and 8 show the vertical profiles of the across-track tangential winds at peak intensity over a 10° radius for all the simulations for the 5 kmCU and 3 kmNoCU simulations, respectively. The profiling is done at peak intensity at height levels between 0 and 18 km and the radial grid extends to 10° for each simulation. The intensification of the TC cases under the future climate scenarios is also shown by the vertical cross-section of the composite of azimuthally averaged winds. Under the SSP5-8.5 scenario, Figs. 7 and 8 show the maximum tangential wind speed increases from 55 to 65 ms^{-1} to up to more than 70 ms^{-1}. This is similar to the result in Manganello et al. (2014) which projects an increase of around 5 ms^{-1} in tangential wind speed on the average for TCs over the WNP. The experiments under future climate scenario also
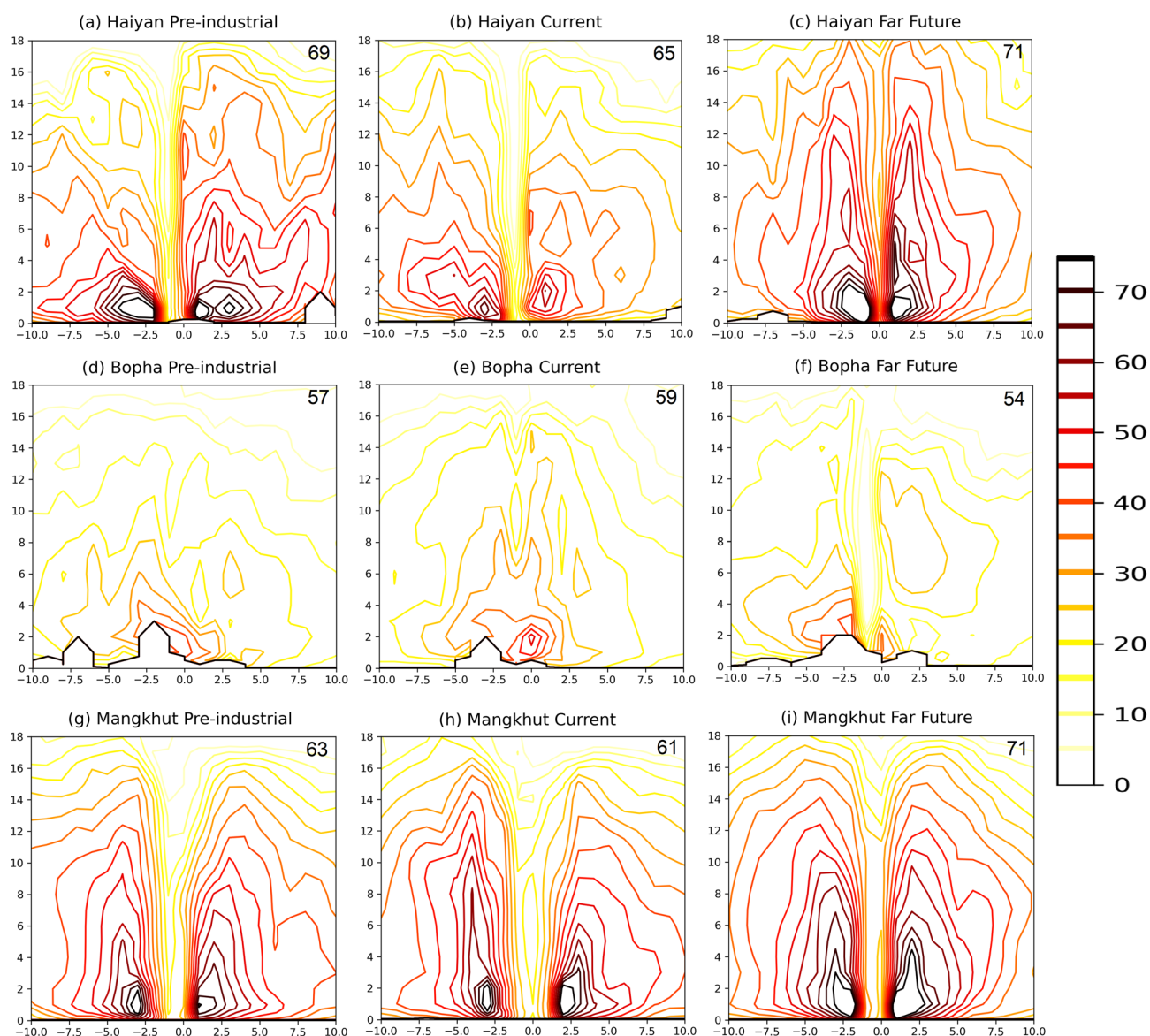
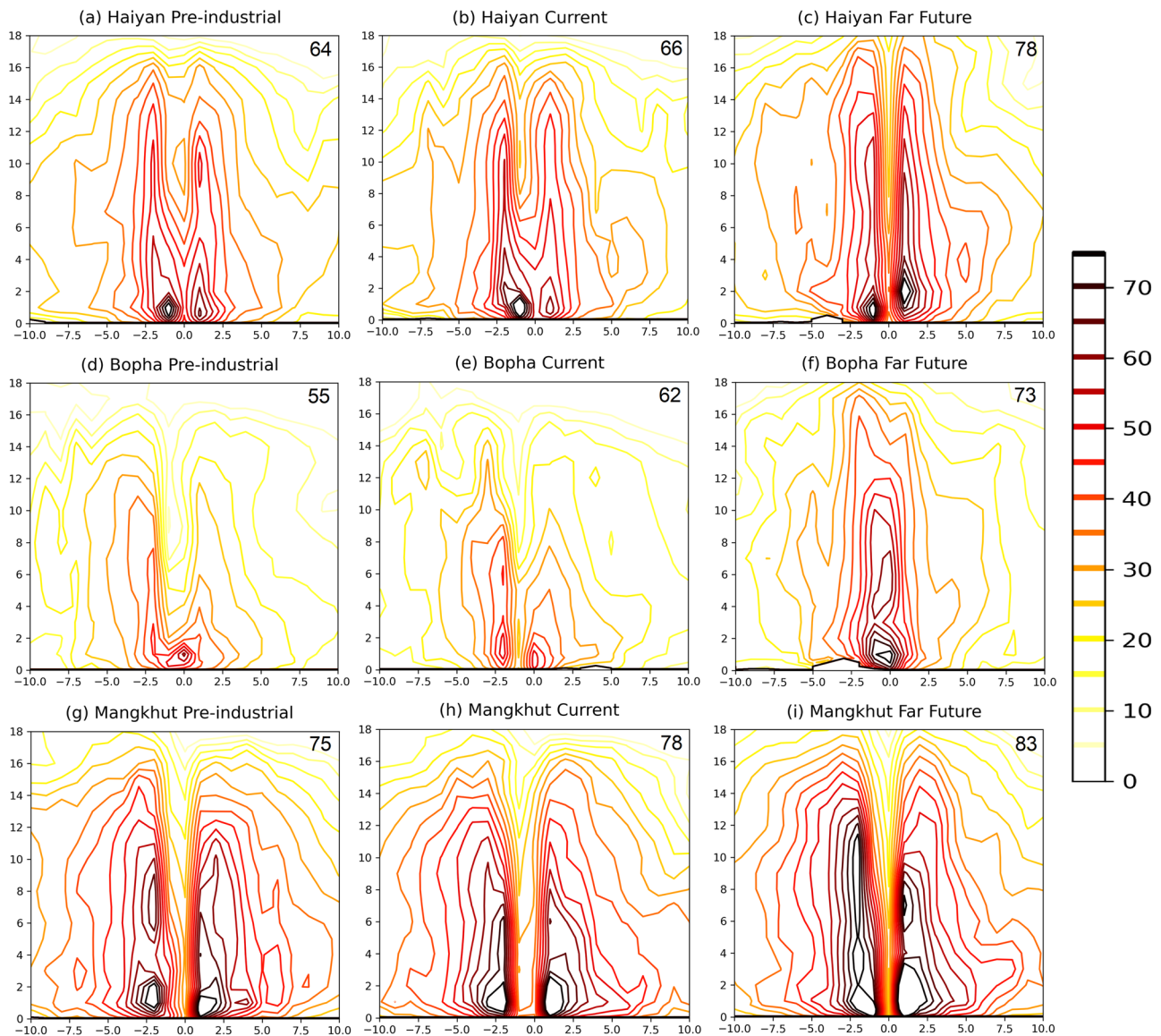**Fig. 7** Radius (in °s) – height (in km) cross sections of tangential (across-track) for Typhoons Haiyan, Bopha and Mangkhut under pre-industrial (left panels), current (middle panels) and future (right pan-els) climate conditions for the 5 kmCU simulations. The number in the right-hand corner indicates the maximum 10-m peak wind intensity in ms^{-1}

project stronger outward and upward expansion of the region of stronger winds. The radial winds also tend to be stronger (inflow) near the surface. Under the pre-industrial climate, the vertical distribution of tangential winds is similar to that of the simulations under the current climate. It is also worthwhile to note here that the vertical distribution of strong tangential winds (> 50 ms^{-1}) increases more in the 3 kmNoCU (Fig. 8) than in the 5 kmCU runs (Fig. 7), for all time periods and three TC cases. This is consistent with the results of an earlier study by Kueh et al. *(2019)* that showed an increase in the vertical extent of stronger tangential wind speeds, a decrease in the outward slope of the maximum wind axis, and a contraction of the eyewall when model grid resolution is increased.

To have a fair comparison between the TC cases under different climate conditions the simulated tracks must be robust and not deviate very much from the observed tracks. Indeed, for both the 5 kmCU and 3 kmNoCU simulations, there are no significant deviations in the track for both pre-industrial and future runs (Supplementary Figs. 4, 5 and 6). In addition, there are no substantial changes in translation speed of all pre-industrial runs in both 5 kmCU and 3 kmNoCU experiments, with percent changes in translation speed ranging from ± 2 m/s. In terms of future projected translation speed, however, there is a small but opposing response between the 5 kmCU and 3 kmNoCU runs, with slower TCs in the 3 kmNoCU ($- 4$ to $- 24\%$)

Fig. 8 Radius (°) – height (in km) cross sections of tangential (across-track) for Typhoon Haiyan, Bopha and Mangkhut under pre-industrial (left panels), current (middle panels) and future (right panels) cli- mate conditions for the 3 kmNoCU simulations. The number in the right-hand corner indicates the maximum 10-m peak wind intensity in ms^{-1}

and faster TCs in the 5 kmCU runs (+ 2 to 9%) under the future climate compared to the current climate sim- ulations. We also found small changes in size, ranging between -7 to 12% in all future runs for all the TC cases in both the 5 kmCU and 3 kmNoCU runs.

3.3 Discussion

In this section we investigated some of the thermodynamic and dynamic aspects from the current, future, and past simu- lations associated with the changes in intensity, size, and speed of the different TC cases.

3.3.1 Intensity

The projected increase in intensity is consistent with the Potential Intensity Theory introduced by Emanuel (1987) based on the Carnot cycle heat engine. According to Ema- nuel (1987), there are two primary factors that control how strong a TC's winds can get – (1) ocean surface temperature and heat content and (2) the temperature and moist state of the atmosphere, thus a TC's potential intensity depends on the moist thermodynamic state of the atmosphere and ocean. Other factors can keep a TC from reaching its poten- tial intensity like vertical wind shear, dry air entrainment and SST cooling from air-sea interaction. If CC increases TC

potential intensity, and other factors counteract this, then it is expected (in theory) that TCs should shift to stronger intensities. Studies like Patricola and Wehner (2018), Bhatia et al. (2018) and Kim et al. (2014) are consistent with this theory.

Based on the results presented in Sect. 3.2.1, there are substantial changes in the intensities in the SFC-only experiments, and more modest increases in the SFC + PLEV and FULL experiments. Such a large intensification is driven by more heat flux supplied from a warmer sea surface in the future. This result agrees with previous studies that demonstrate the important role of warm SST on TC intensification (Delfino et al. 2022b; Chen et al. 2020; Nakamura et al. 2016). On the other hand, as can be seen in the SFC + PLEV and FULL experiments, atmospheric warming has a large negative impact on TC intensity, but the TC cases still increased intensity under the future climate. Some previous studies have also pointed out that atmospheric warming itself can weaken TCs, due to the associated increase in atmospheric stability (Chen et al. 2020; Nakamura et al. 2016). Additionally, although the relative humidity is slightly increased under the future climate, the FULL experiments (with relative humidity changes) show no significant difference from the SFC + PLEV experiments, consistent with Parker et al. (2018) and Chen et al. (2020).

From the results presented in Sect. 3.2.2, we have seen increases in intensity under the future simulations. Based on maximum potential intensity theory (Emanuel 1987) and recent studies (Patricola and Wehner 2018, Nakamura

et al. 2016, Chen et al. 2020, Mittal et al. 2019, Parker et al. 2018), TC intensity is expected to increase due to favorable conditions such as warmer ocean temperature, unstable atmosphere with a moist mid-troposphere, and weak vertical wind shear (Wu et al. 2022). Figures 9 and 10 shows increases in both the water vapor mixing ratio and latent heat flux under the SSP5-8.5 scenario in the future climate. The water vapor mixing ratio increase is 32% (66%), 27% (29%), and 26% (29%) under the future climate condition in the 5 kmCU (3 kmNoCU) experiments (Table 8). The increase in latent heat flux is 10% (30%), 16% (30%), and 5% (1%) under the 5 kmCU (3 kmNoCU) for Typhoons Haiyan, Bopha and Mangkhut, respectively (Table 8). This is also similar to the results of Gutmann et al. (2018) which showed that the increases in water vapor and thus latent heat feedbacks lead to increases in TC intensity. In the future climate, TCs may have a deeper TC core due to enhanced latent heating from increased precipitation and a significant decrease in the vertical wind shear (Mittal et al. 2019). The intensification may be driven by more latent heat flux supplied from a warmer ocean in the future (Chen et al. 2020; Nakamura et al. 2016) and due to the change to the SST gradient (Parker et al. 2018).

The observed changes in the vertical profile of temperature in a moist environment with enhanced SST will increase the convective available potential energy (CAPE) (Trenberth 2005). The CAPE values are also calculated, where a notable increase is seen in the far future scenarios for all
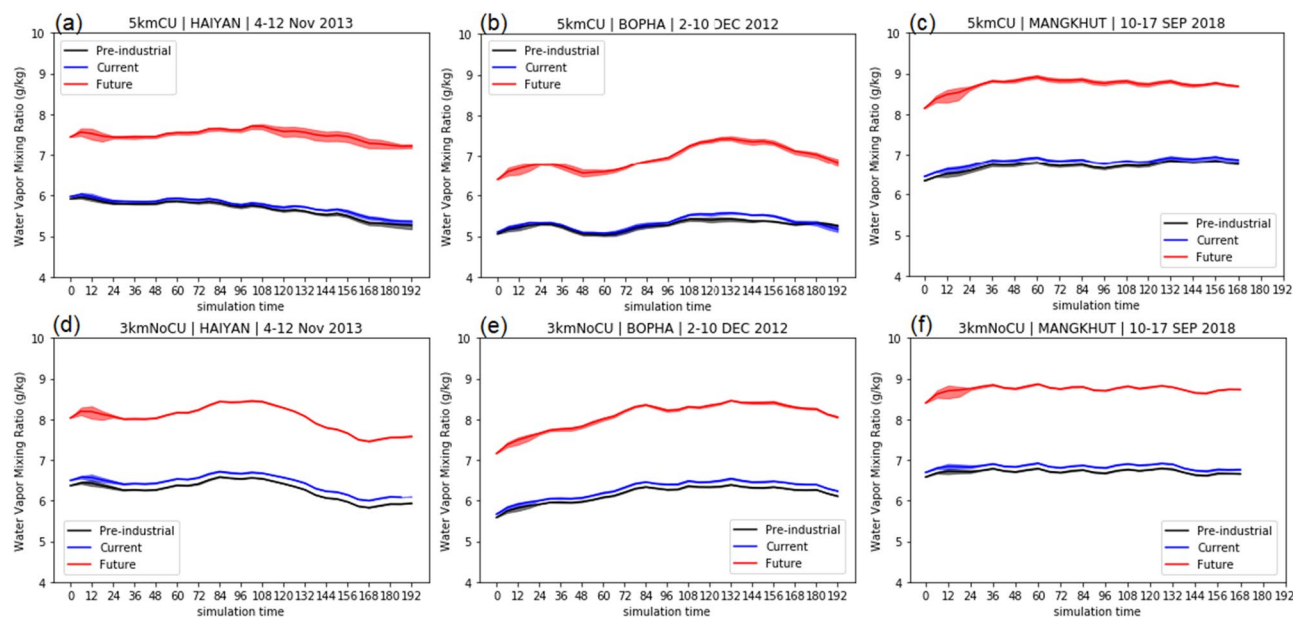
Fig. 9 Simulated water vapor mixing ratio (g/kg), averaged over the domain, from the 5 kmCU (top panels) and 3 kmNoCU (bottom panels) experiments under pre-industrial (black), current (blue) and future (red) climate for the different TC case studies—(**a, d**) Haiyan (left), (**b, e**) Bopha (center) and (**c, f**) Mangkhut (right). Solid lines denote the mean, and the spread denotes the simulated intensity from the four ensemble members initialized at different times
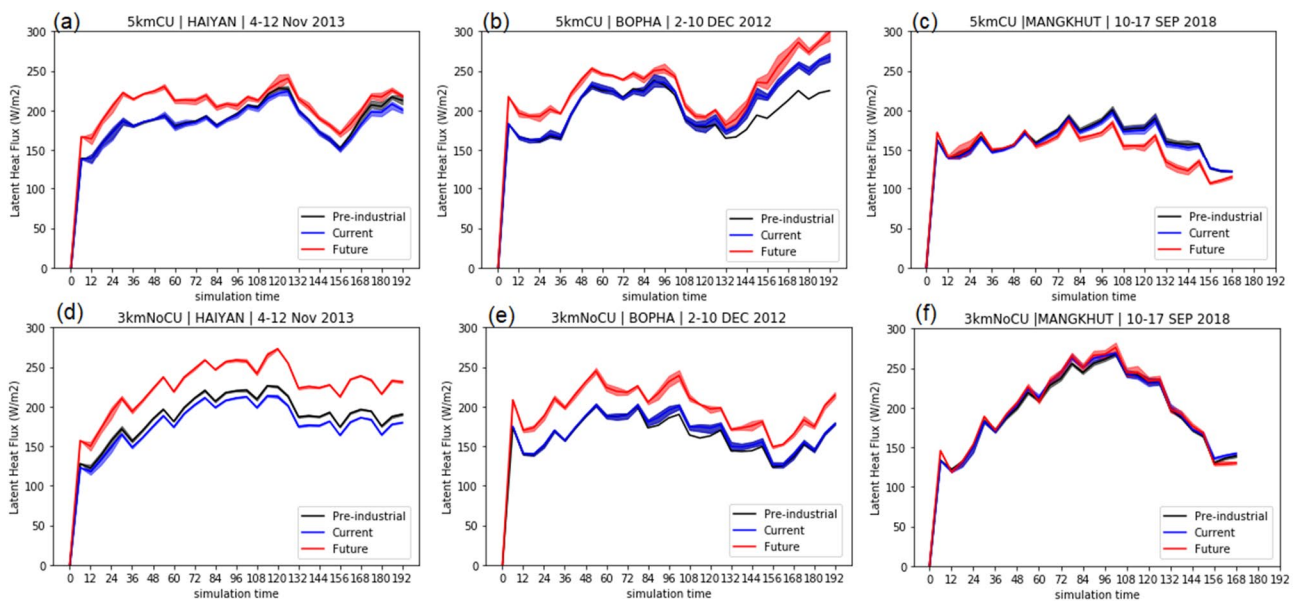
Fig. 10 Simulated latent heat flux (W m-2), averaged over the domain, from the 5 kmCU (top panels) and 3 kmNoCU (bottom panels) experiments under pre-industrial (black), current (blue) and future (red) climate for the different TC case studies—(**a**, **d**) Haiyan (left), (**b**, **e**) Bopha (center) and (**c**, **f**) Mangkhut (right). Solid lines denote the mean, and the spread denotes the simulated intensity from the four ensemble members initialized at different times

the TCs considered. There is a 41% (45%), 37% (51%), and 44% (36%) average increase in CAPE in the far future SSP5-8.5 scenario for the 5 kmCU (3 kmNoCU) simulations for Typhoons Haiyan, Bopha and Mangkhut, respectively. This increase in CAPE values in future climate is consistent with previous studies (Knutson and Tuleya 2004; Parker et al. 2018). The higher CAPE enhances the potential for more vigorous atmospheric convection and further intensifies TCs (Knutson and Tuleya 2004; Reddy et al. 2019). A warmer and moist environment with high SSTs is observed in the November (2.73) and September (2.75) climate change signal than in December (2.63) under the SSP5-8.5 (see in Fig. 2). Hence, TCs Haiyan and Mangkhut are seen to

intensify more with substantial relative changes in CAPE compared to Bopha in the future climate (Fig. 11).

Vertical wind shear is also a critical factor in both TC formation and intensification. The reduction in vertical wind shear is favorable to the formation and development of TCs. There is a reduction in the vertical wind shear (between 850 and 200 hPa) on average (Fig. 12) across the domain. The vertical wind shear across the domain is reduced under the future climate of about -2%, -2%, and -4% for Haiyan, Bopha, and Mangkhut, respectively for the 5 kmCU experiments. For the 3 kmNoCU experiments, the reduction in vertical wind shear is -4%, -3%, and -6% for Haiyan, Bopha, and Mangkhut, respectively.

Table 7 Summary of ensemble mean changes (difference) in minimum central pressure (in hPa) and maximum 10-m wind speed (in ms^{-1}) between the current and preindustrial/future climate simula-tions. Ensemble mean changes denoted by * are significant at the 10% level, by ** are significant at the 5% level and by *** are significant at 1% confidence level using a Student's t test

Simulation Group/Code	Periods	Haiyan		Bopha		Mangkhut	
		Minimum central pressure (hPa)	Maximum Wind (ms^{-1})	Minimum central pressure(hPa)	Maximum Wind (ms^{-1})	Minimum central pressure (hPa)	Maximum Wind (ms^{-1})
5 kmCU	Current—preind	10	− 4	− 9***	4	0	0
	Future—current	− 4|*	3*	− 1	2	− 11***	8***
3 kmNoCU	Current—preind	− 1	2	− 19***	10***	− 3**	2*
	Future—current	− 20***	9***	− 4**	3***	− 10***	9***

Table 8 Summary of mean percent changes (future minus current climate/current and current minus pre-industrial/pre-industrial) in TC Environment for the 5 kmCU and 3 kmNoCU experiments

TC environment	Periods	HAIYAN		BOPHA		MANGKHUT	
		5 kmCU	3 kmNoCU	5 kmCU	3 kmNoCU	5 kmCU	3 kmNoCU
Sensible heat flux	Future– current	− 25%	− 16%	− 18%	− 9%	− 27%	− 31%
	Current-pre-industrial	− 4%	− 5%	5%	7%	− 1%	1%
Latent heat flux	Future-current	10%	30%	16%	30%	5%	1%
	Current-pre-industrial	− 7%	− 6%	9%	1%	6%	− 5%
Water vapor mixing ratio	Future-current	32%	66%	27%	29%	26%	29%
	Current-pre-industrial	2%	− 23%	− 7%	− 6%	2%	2%
Mid-tropospheric Relative Humidity	Future-current	− 4%	4%	1%	1%	5%	2%
	Current-pre-industrial	2%	3%	2%	2%	0%	− 1%
Vertical wind shear	Future-current	− 2%	− 4%	− 2%	− 3%	− 4%	− 6%
	Current-pre-industrial	3%	− 3%	0%	2%	1%	4%
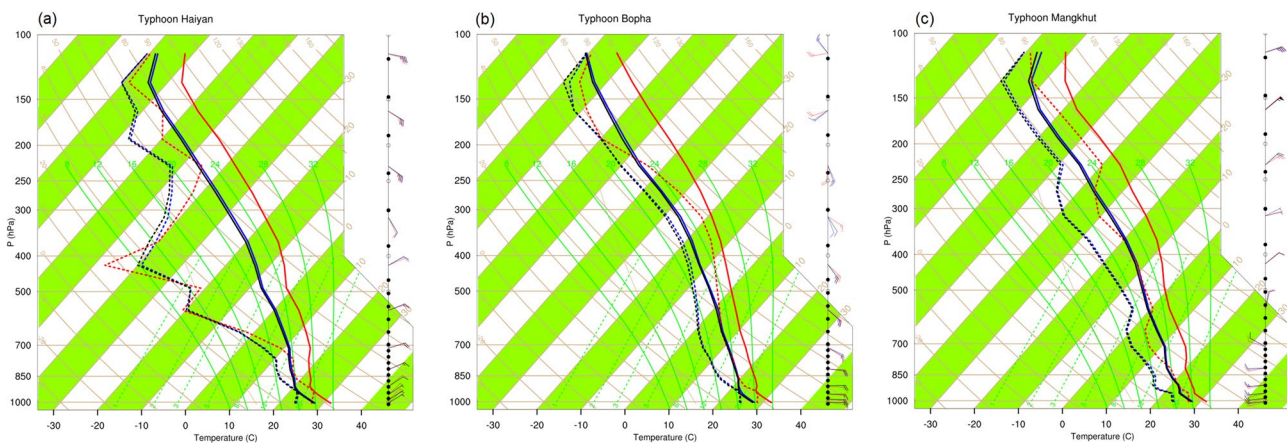
Fig. 11 Vertical profile of air temperature (solid line) and dew point temperature (dashed line) of Typhoons Haiyan (**a**), Bopha (**b**) and Mangkhut (**c**) for the future (red line) SSP5-8.5 and pre-industrial (black line) scenarios considered in this study along with comparisons with the control run (blue line)

3.3.2 Track and translation speed

Based on the results presented in Sect. 3.2.1 above, there are substantial changes in the TC track under the SFC-only experiments for all three TC cases (Supplementary Fig. 4). We have also found that the SFC-only experiments, where the tracks recurved, had an enhanced westerly steering flow as well as a retracted Western North Pacific Subtropical High (WNPSH). This is consistent with previous studies, which showed that the TC track can be altered due to the changes in TC size as well as in the retraction of the WNPSH (Sun et al. 2015, 2017). On the other hand, the SFC + PLEV and FULL in the 5 kmCU experiments did not show any significant changes in the TC track. In addition, based on the results presented in Sect. 3.2.2, there are minimal changes in the TC track due to small changes in the steering flow in th3 3 kmNoCU experiments (Supplementary Figs. 5, 6, 7).

The observed and future changes in TC translation speed remain uncertain (Zhang et al. 2020; Yamaguchi et al. 2020), primarily due to lack of studies and clear evidence (Kossin 2021). In this study, we found minimal changes (± 2 ms^{-1}) in translation speed with opposing signals from the 5 kmCU (faster) and 3 kmNoCU (slower). However, the changes in the large-scale atmospheric circulation patterns as well as the recurrent modes of climate variability affecting the WNP are not considered here, thus, the future changes in tracks and translation speeds are not fully accounted for.

3.3.3 Size

Larger TC size is found to be due to an increase in environmental humidity and temperature in the lower-troposphere leading to an increase in environmental CAPE (Mittal et al. 2019). Although the changes in mid-tropospheric RH are
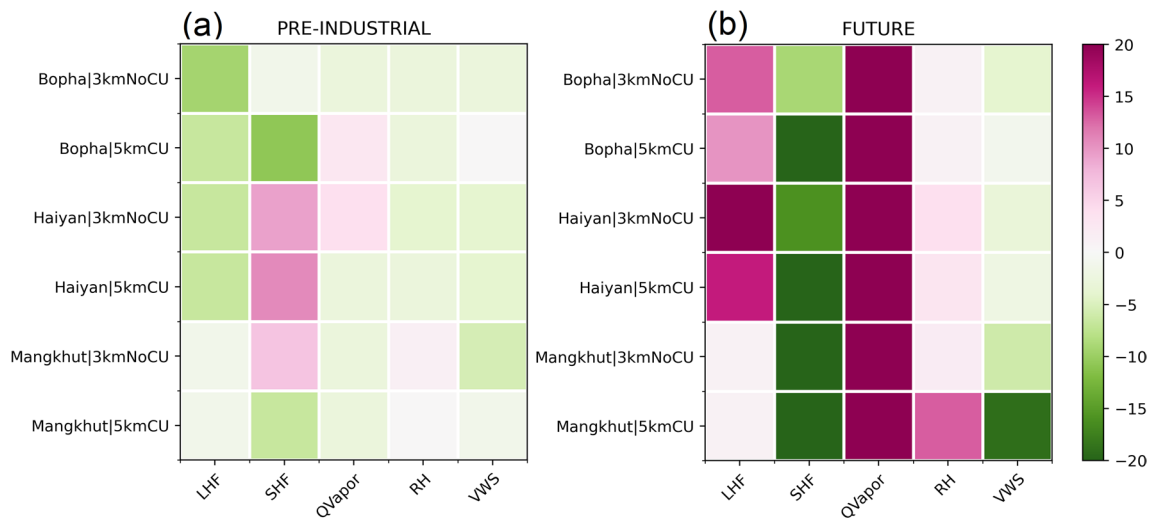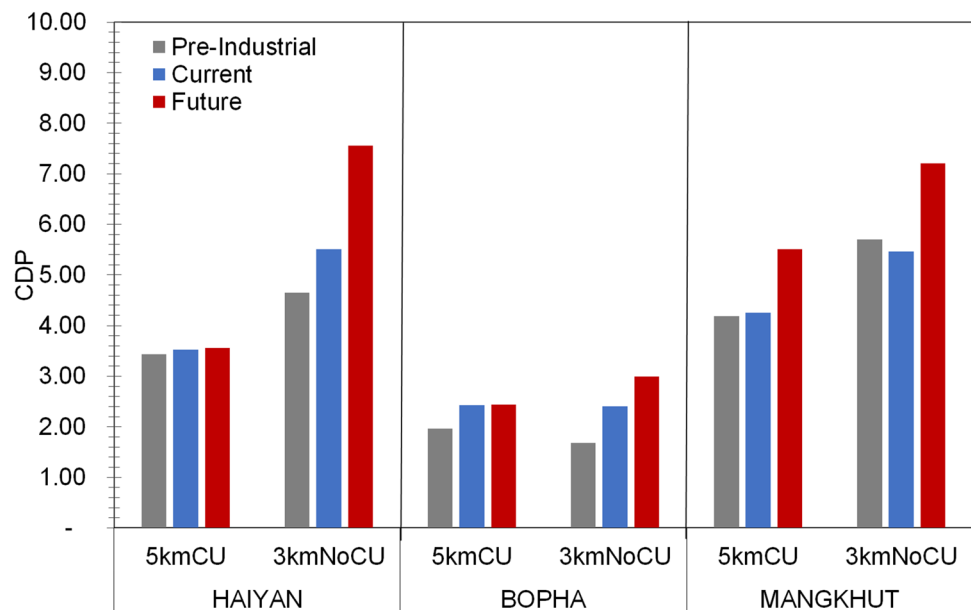
Fig. 12 Percent change relative to the current climate in latent (LHF) and sensible heat flux (SHF), water vapor mixing ratio (QVapor), relative humidity (RH) and vertical wind shear (VWS) averaged across the domain over the simulation period for the 5 kmCU and 3 kmNoCU experiments for Typhoon Haiyan, Bopha, and Mangkhut under pre-industrial (a) and future (b) climate
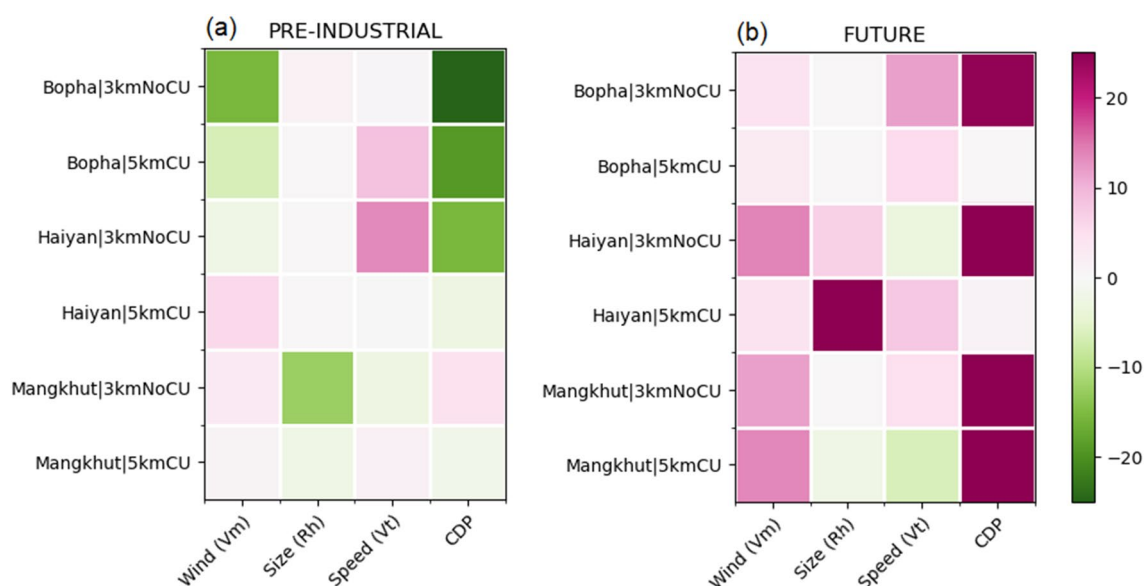
Fig. 13 Cyclone Damage Potential (CDP) of the 5 kmCU and 3 kmNoCU experiments for Typhoon Haiyan, Typhoon Bopha, and Typhoon Mangkhut under the pre-industrial (gray), current (blue) and future (red) climate

minimal (between 1 to 13%) in all three cases, the RH are higher under future climate conditions relative to the current climate. This might explain the relatively small changes in size. There is also a relatively similar response between 5 kmCU and 3 kmNoCU experiments. In addition, there is also an increase in the mid-tropospheric RH in all three cases Haiyan, Bopha, and Mangkhut. The high mid-tropospheric RH supports TC development and intensification by restricting the negative influence on convection (Gray 1998).

3.3.4 Summary of discussion

Figure 12 and Table 8 show the summary of the percent changes in the TC environment under the pre-industrial and future climate, relative to the current climate simulations. The changes in latent heat flux for the 5 kmCU (3 kmNoCU) runs ranges between 5% (5%), – 7% (– 5%), and 1% (– 1%) for Typhoons Haiyan, Bopha, and Mangkhut under the pre-industrial climate, while under SSP5-8.5 scenario in the future climate, the latent heat flux changes range from 10% (30%), 16% (30%), and 5% (1%) for the 5 kmCU (3 kmNoCU) runs of Typhoons Haiyan, Bopha, and

Fig. 14 Percent change in TC characteristics relative to the current climate of the Cyclone Damage Potential (CDP) and individual parameters: maximum winds (Vmax), radius of hurricane force wind (HFWrad or Rh) and translation speed (TS) of the 5 kmCU and 3 kmNoCU experiments for Typhoon Haiyan, Typhoon Bopha, and Typhoon Mangkhut under the pre-industrial climate (left) and future climate (right)

Mangkhut, respectively. The water vapor mixing ratio also increased in the future with changes ranging from 26 to 35% for the 5 kmCU runs and 29% to 66% for the 3 kmNoCU runs. There is a general decrease in the vertical wind shear which ranges from − 2% (− 4%), − 2% (− 3%), and − 4% (− 6%) for the 5 kmCU (3 kmNoCU) runs for Typhoons Haiyan, Bopha, and Mangkhut, respectively. These changes in the TC environment, particularly the increase in latent heat flux and water vapor mixing ratio; and the reduction in vertical wind shear, appear to be the main contributors to the further intensification of the TC cases in the future climate simulations.

The increase in atmospheric convective instability in the TC outer region below the middle troposphere, which facilitates the local development of grid-scale ascending motion, low-level convergence, and the acceleration of tangential winds, may be responsible for the TC size response to ocean warming. A rise in environmental humidity and temperature in the lower troposphere leads to an increase in environmental CAPE, resulting in larger TC size (Mittal et al. 2019).

3.4 Cyclone damage potential

Overall, there is higher damage potential in the future for all three TC cases and in both the 5 kmCU and 3 kmNoCU simulations (Fig. 13). The increase in CDP ranges from 3.56, 2.43, and 5.50 for the 5 kmCU runs; and 7.55, 2.99, and 7.21 for the 3 kmNoCU runs under the far future SSP5-8.5 scenario. Under the pre-industrial (current) climate, the TC

cases' CDP ranges from 3.43 (3.53), 1.97 (2.43), and 4.18 (4.25) for the 5 kmCU runs; and 4.65 (5.51), 1.67 (2.40), and 5.70 (5.46) for the 3 kmNoCU runs for Typhoons Haiyan, Bopha, and Mangkhut, respectively. The increase in CDP is primarily due to the increase in maximum winds, with small changes in both size and speed. The changes in CDP are generally larger in the 3 kmNoCU runs than in the 5 kmCU runs with changes ranging from + 1%, + 0.17%, and + 30% for the 5 kmCU runs and + 37%, + 25%, and + 32% in the 3 kmNoCU runs for Typhoons Haiyan, Bopha, and Mangkhut, respectively. Under the pre-industrial climate, however, there are minimal changes in the CDP for Typhoons Haiyan and Mangkhut, ranging between − 3 to − 15% (pre-industrial minus current), but for Typhoon Bopha the change in CDP is − 19% (− 30%) in the 5 kmCU (3 kmNoCU) runs showing that Typhoon Bopha had more damage potential under the current climate as compared to if it happened in the past.

The percent changes in the damage potential of the different TC cases relative to the current are presented in Fig. 14. Typhoons Haiyan, Bopha, and Mangkhut's maximum winds increased under future climate conditions in both 5 kmCU and 3 kmNoCU simulations. Changes in size are relatively small and have mixed signal of responses, with increases/decreases for different TC case and in 5 kmCU and 3 kmNoCU simulations. The 5 kmCU experiments led to a change of + 30%, − 11%, and − 2% for Haiyan, Bopha and Mangkhut, respectively and the 3 kmNoCU experiments led to 0%, 6.67%, and 0% change for Haiyan, Bopha

and Mangkhut. Under the pre-industrial climate, Haiyan did not show any change in the TFW and DFW under the 3 kmNoCU and 5 kmCU simulations, Bopha showed minimal changes, but Mangkhut showed up to – 13% and – 2% change in TFW under the 3 kmNoCU and 5 kmCU simulations (Fig. 14).

We also computed the changes in the translation speed of the TC cases since the future changes in speed remain uncertain. For the translation speed, we find an opposite signal of responses i.e., the TC cases move slower in 3 kmNoCU with – 24%, – 10%, and – 4% and faster in the 5 kmCU simulations with 6%, 10%, and 4% change in speed for Typhoons Haiyan, Bopha, and Mangkhut, respectively (Fig. 14). Under the pre-industrial climate, the TCs response in terms of speed have changes of 18% for Haiyan, – 1% for Bopha, and – 2% for Mangkhut in the 3 kmNoCU runs. Additional work is needed to achieve more generalized conclusions over the TC response in terms of size and speed.

4 Summary and conclusions

The Weather Research and Forecasting (WRF) Model was used to simulate the potential impacts of large-scale environmental changes due to global warming on the simulation of three of the most damaging TC events in the Philippines. A set of simulations using 5 km resolution inner domain with cumulus scheme (5 kmCU), and a 3 km resolution domain without cumulus parameterization (3 kmNoCU), for four different initial times in each TC case, were able to capture the observed track and intensity of Typhoons Haiyan, Bopha, and Mangkhut.

The PGW technique was used to explore the response of the TC cases to historical and future warming climate. By using forcings from four different CMIP6 GCMs, the current weather patterns during the period of the TC events were re-simulated under different future (past) climates. The current, pre-industrial and future were computed from the monthly mean values obtained from the different GCMs, with the SSP5-8.5 scenario in the future. Based on the future climate change signals calculated from these four GCMs, the mean SST change is projected to be between 1.89 °C to 3.65 °C warmer and the air temperature will be ~ 3 °C to 6 °C warmer on the average, with stronger warming in the upper level (near 250 hPa), leading to the atmosphere being more stable in the future under SSP5-8.5 scenario. The relative humidity in the troposphere, particularly in the mid-troposphere, shows a minimal change in the future climate under the SSP5-8.5 scenario.

Based on the results for the far future SSP5-8.5 scenarios, we have found that the intense TC events would be even more intense in the future, with significant increases in maximum peak winds and reduction minimum central pressure in both 5 kmCU and 3 kmNoCU runs. Previous studies that have done similar kinds of work for TCs from different basins (Patricola and Wehner 2018), for three TC cases in the Pearl River Delta (Chen et al. 2020), Bay of Bengal (Mittal et al. 2019), and Australia (Parker et al. 2018) has also reported mostly increases in peak intensity, particularly maximum winds. There are also higher rates of intensity change if we consider surface warming only, while atmospheric warming offsets the intensification caused by surface warming only, consistent with Nakamura et al. (2016) and Chen et al. (2020). Our study further found that in the future, the increase in intensity is mainly due to warmer temperatures, higher latent heat fluxes, increased water vapor mixing ratio, and less vertical wind shear. In addition, under the future climate, the more intense TCs like Haiyan and Mangkhut would have a deeper TC core or greater vertical extent of stronger winds primarily due to enhanced latent heating.

The results also show relatively small changes in track and translation speed in the future simulations compared to the current simulations, due to small changes in the TC steering flow. In fact, the TCs are slightly faster (slower) with an average of + 6% (– 24%), + 10% (– 10%), and + 4% (– 4%) for Typhoons Haiyan, Bopha and Mangkhut in the 5 kmCU (3 kmNoCU) simulations compared to the current runs. Our study also found small changes in size, ranging between – 7 to 12% in all future runs for all the TC cases, which might potentially add insights to the general lack of studies on the response of TC size to future warming (Kossin 2021).

By comparing with the current simulations, the simulations under the pre-industrial climate showed that climate change has so far weakly influenced the intensity of the TC cases but did not have much influence on the TC cases' track, translation speed, and size. With the increase in maximum winds, the damage potential of Haiyan and Mangkhut are slightly increased in the current climate simulations than the pre-industrial climate simulations. More importantly, the TC cases are expected to further intensify with continued warming in the future under the SSP5-8.5 scenario simulations compared to the current climate. The 3 kmNoCU simulations have the same sign of projected changes in TC intensity with the 5 kmCU simulations, with different responses in size and speed among the simulations. These results suggest that convective parameterization introduces minimal uncertainty in terms of TC intensity, however, TC speed and size need further investigation.

It is very important to note here that there is a range of responses i.e., signal and magnitude of change from different TC cases and GCM forcings. This highlights the uncertainty due to the potential range of sensitivities brought about by different models. However, the changes in intensity in the

simulations forced by GCMs with higher mean SST deltas (CESM2 and HadGEM3) and lower mean SST deltas (MPI and MIROC6) do not show systematic differences. This highlights the uncertainties associated with the use of different GCMs and TC cases, which have been lacking in similar studies that used the PGW technique to investigate the response of TCs to climate change. These past studies did not investigate the uncertainties associated with the use of different GCMs (Parker et al. 2018; Patricola and Wehner 2018; Mittal et al. 2019; Reddy et al. 2021). Past studies have highlighted the need for and importance of studying multiple TC cases (Nakimura et al. 2016; Parker et al. 2018; et al. Mittal et al. 2019) with varying TC intensities (Nakamura et al. 2016) and in different seasons, to identify outliers in TC response to future climate conditions (Parker et al. 2018), which we have attempted to address in this study. Therefore, the novelty in our study is in investigating (1) simulations forced with initial and boundary conditions from several GCMs; (2) the sensitivity to the use of different cumulus schemes and initialization times (Delfino et al. 2022a); (3) using WRF's simple mixed-ocean layer model in order to capture the atmosphere–ocean feedback during the passage of TCs; and (4) different TC cases with observed varying intensity, landfall area, & months of occurrence. In addition, this study also tries to address the lack of attention of past studies to the physical mechanisms involved (Wu et al. 2022). We attempted to identify the physical mechanisms driving the simulated TC responses and discuss relevant underlying uncertainties.

However, there are still some aspects of the results of this study that need to be interpreted with caution due to (1) the limitations of the PGW technique i.e. it does not address the uncertainties surrounding the different modes of climate variability that are relevant in TC activity; (2) the small sample-size of the TC cases; and (3) it does not account for the range of uncertainty associated with the use of different limited area models and reanalysis datasets as initial and boundary conditions. The use of a single limited area model (WRF) for three TC cases and different GCM forcings allowed us to assess the robustness of the TC responses to future and past climate more directly among the TC cases and the different GCM forcings. However, the uncertainty in relation to the use of different limited area models is not within the scope of this study and can be an important aspect to look at in future studies. Global and regional modeling initiatives such as Coordinated Regional Climate Downscaling Experiment (CORDEX) could help address this uncertainty. Whilst the PGW method is useful to provide more detail of TC properties and their possible changes than global simulations, it cannot account for the remote influence of the large-scale atmospheric circulation patterns or the recurrent modes of climate variability affecting the WNP that can affect the steering flow of the TCs. This means that any changes seen in the tracks and translation speeds must be considered with caution. In addition, any large changes in track in the SFC-only experiments mean the TCs will no longer experience the original environment modified by the climate change delta/SST anomalies.

In conclusion, based on our simulations of the different TC cases using the PGW approach, it is found that the most damaging TCs like Haiyan, Bopha, and Mangkhut will have higher damage potential in the future. The increase in the CDP ranges from ~1% to up to 37% in the future under the SSP5-8.5 scenario, primarily due to the increase in maximum winds. TCs of such intensity and damage potential in the future will have serious implications with the increasing exposure and vulnerability in the Philippines.

Declarations

Conflict of interest The authors have no relevant financial or non-financial interests to disclose.

Ethics approval and consent to participate Not applicable.

Consent for publication Not applicable.

Availability of data and material Simulation data are stored at the JASMIN data storage facility and are available upon request from the corresponding author. Code for the WRF model is available at http://www.www2.mmm.ucar.edu/wrf/users/downloads.html. WPS geographical input data are available from https://www.www2.mmm.ucar.edu/wrf/users/download/get_sources_wps_geog.html#mandatory. TRACK is available from https://www.gitlab.act.reading.ac.uk/track/45track. CF-python and CF-plot were used in the analysis and visualization, and installation packages are available from https://www.ncas-cms.github.io/cf-python/.

References

Adachi SA, Tomita H (2020) Methodology of the constraint condition in dynamical downscaling for regional climate evaluation: A review. J Geophys Res-Atmos 125 e2019JD032166

Aragon LGB, Pura AG (2016) Analysis of the displacement error of the WRF–ARW model in predicting tropical cyclone tracks over the Philippines. Met Apps 23:401–408

Bagtasa G (2021) Analog forecasting of tropical cyclone rainfall in the Philippines. Weather Clim Extremes 32:100323

Bengtsson L, Hodges K, Esch I, Keenlyside M, Kornblueh N, Luo L, J-J and Yamagata T, (2007) How may tropical cyclones change in a warmer climate? Tellus a: Dyn Meteorol Oceanogr 59(4):539–561

Bhatia K, Vecchi G, Murakami H, Underwood S, Kossin J (2018) Projected response of tropical cyclone intensity and intensification in a global climate model. J Clim 31(20):8281–8303

Bruyère PCL, C L Mooney P A & Lynch A H, (2018) The response of land-falling tropical cyclone characteristics to projected climate change in northeast Australia. Clim Dyn 51(9):3467–3485

Camargo SJ, Wing AA (2016) Tropical cyclones in climate models. Wires Clim Chang 7:211–237

Chen J, Wang Z, Tam C, Lau N, Lau D, D & Mok H, (2020) Impacts of climate change on tropical cyclones and induced storm surges in the Pearl River Delta region using pseudo-global- warming method. Sci Rep 10(1):1–10

Christensen et al (2013) Climate phenomena and their relevance for future regional climate change. In: Stocker et al eds Climate Change 2013: The Physical Science Basis Contribution of Working Group I to the Fifth Assessment Report of the Intergovernmental Panel on Climate Change (IPCC AR5) Cambridge UK and New York NY: Cambridge University Press

CPC (Climate Prediction Center) (2021) Cold and Warm Episodes by Season. https://www.origincpcncepnoaagov/products/analysis_monitoring/ensostuff/ONI_v5php

Cruz F, Narisma G (2016) WRF simulation of the heavy rainfall over Metropolitan Manila Philippines during tropical cyclone Ketsana: a sensitivity study. Meteorol Atmospheric Phys 128(4):415–428

Dai A, Rasmussen RM, Ikeda K et al (2020) A new approach to construct representative future forcing data for dynamic downscaling. Clim Dyn 55:315–323

Daron J, Macadam I, Kanamaru H, Cinco T, Katzfey J, Scannell C, Daron J (2018) Providing future climate projections using multiple models and methods: insights from the Philippines. Clim Chang 148(1):187–203

Daron J, Macadam I, Gallo F, Buonomo E, Tucker S (2016) Building resilience to climate extremes following typhoon Haiyan in the Philippines Work package 3 technical report: methodological approach and results for HadGEM3-RA climate projections Exeter: Met Office Available at: http://www.precisrcmcom/DFID_Philippines_Reporting/WP3_Technical_Report_final_07-12-2016pdf

Delfino RJP, Bagtasa G, Vidale PLV, Hodges K (2022a) Sensitivity of simulating Typhoon Haiyan (2013) using WRF: the role of cumulus convection surface flux parameterizations spectral nudging and initial and boundary conditions. Nat Hazards Earth Syst Sci 22:3285–3307

Delfino RJP, Hodges K, Vidale PLV, Bagtasa G (2022b) Sensitivity of tropical cyclone simulations to sea surface and atmospheric temperature forcing: cases from the Philippines. Under review.

Danabasoglu G, Lamarque J-F, Bacmeister J, Bailey DA, DuVivier AK, Edwards J, Emmons LK, Fasullo J, Garcia R, Gettelman A, Hannay C, Holland MM, Large WG, Lauritzen PH, Lawrence DM, Lenaerts JTM, Lindsay K, Lipscomb WH, Mills MJ, Neale R, Oleson KW, Otto-Bliesner B, Phillips AS, Sacks W, Tilmes S, Kampenhout L, Vertenstein M, Bertini A, Dennis J, Deser C, Fischer C, Fox-Kemper B, Kay JE, Kinnison D, Kushner PJ, Larson VE, Long MC, Mickelson S, Moore JK, Nienhouse E, Polvani L, Rasch PJ, Strand WG (2020) The Community Earth System Model Version 2 (CESM2) Journal of Advances in Modeling Earth Systems 12(2). https://doi.org/10.1029/2019MS001916

Done JM, PaiMazumder D, Towler E, Kishtawal CM (2018) Estimating impacts of North Atlantic tropical cyclones using an index of damage potential. Clim Change 46:561–573

Emanuel K (1987) The dependence of hurricane intensity on climate. Nature 326:483–485

Emanuel K (2020) Response of Global Tropical Cyclone Activity to Increasing CO2: Results from Downscaling CMIP6 Models. J Clim 34(1):57–70

Eyring V, Bony S, Meehl GA, Senior CA, Stevens B, Stouffer RJ, Taylor KE (2016) Overview of the Coupled Model Intercomparison Project Phase 6 (CMIP6) experimental design and organization. Geosci Model Dev 9:1937–1958

Flores RA (2019) Geovisual Analytics on the verification of the PAGASA Numerical Weather Prediction Model Rainfall Forecast. Int Arch Photogramm Remote Sens Spatial Inf Sci XLII-4/W19 215–

Gallo F, Daron J, Macadam I, Cinco T, Villafuerte M, Jones R, G … Tucker S, (2019) High-resolution regional climate model projections of future tropical cyclone activity in the Philippines. J Int J Climatol 39(3):1181–1194

Gray WM (1998) The Formation of Tropical Cyclones. Meteorol Atmospheric Phys 67(1):37–69

Gutmann ED, Rasmussen RM, Liu C, Ikeda K, Bruyere CL, Done JM, Garrè L, Friis-Hansen P, Veldore V (2018) Changes in hurricanes from a 13-yr convection-permitting pseudo–global warming simulation. J Clim 1 31(9):3643–3657

Hersbach H, Bell B, Berrisford P, Hirahara S, Horányi A, Muñoz-Sabater J, Nicolas J, Peubey C, Radu R, Schepers D, Simmons A(2020) The ERA5 global reanalysis. Q J Roy Meteorol Soc 146(730):1999–2049

Hill KA, Lackmann GM (2011) The impact of future climate change on TC intensity and structure: a downscaling approach. J Clim 24:4644–4661

Hodges K, Cobb A, Vidale PL (2017) How well are tropical cyclones represented in reanalysis datasets? J Clim 30(14):5243–5264

Hodges KI, Klingaman NP (2019) Prediction errors of tropical cyclones in the western north Pacific in the Met Office global forecast model. Weather Forecast 34(5):1189–1209

Holland GJ, Done J, Bruyere C, Cooper C, Suzuki A (2010) Model investigations of the effects of climate variability and change on future Gulf of Mexico tropical cyclone activity. In: Proc Offshore Technology Conf Houston 20690

Holland GJ JM Done M Ge and R Douglas (2016) An Index for Cyclone Damage Potential. https://www.amsconfexcom/ams/32Hurr/webprogram/Paper293660html

Isaksen L, Bonavita M, Buizza R, Fisher M, Haseler J, Leutbecher M, Raynaud L (2010) Ensemble of data assimilations at ECMWF

Islam T, Srivastava PK, Rico-Ramirez MA et al (2015) Tracking a tropical cyclone through WRF–ARW simulation and sensitivity of model physics. Nat Hazards 76:1473–1495

Judt F, Klocke D, Rios-Berrios R, Vanniere B, Ziemen F, Auger L, Biercamp J, Bretherton C, Chen X, Duben P, Hohenegger C, Kharaidnutov M, Kodama C, Kornblueh L, Nakano L-J, Neumann M, Putman P, Rober W, Roberts N, Satoh M, Shibuya M, Stevens R, Vidale B, P L Wedi N and Zhou L, (2021) Tropical cyclones in global storm-resolving models. J Meteorol Soc Japan Ser II 99(3):579–602

Kain JS (2004) The Kain-Fritsch convective parameterization: an update. J Appl Meteorol Climatol 43:170–181

Kawase H, Yoshikane T, Hara M, Kimura F, Yasunari T, Ailikun B, Ueda H, Inoue T (2009) Intermodel variability of future changes in the Baiu rainband estimated by the pseudo global warming downscaling method. J Geophys Res Atmos 114(D24)

Kawase H, Yamaguchi M, Imada Y, Hayashi S, Murata A, Nakaegawa T, Miyasaka T, Takayabu I (2021) Enhancement of extremely heavy precipitation induced by Typhoon Hagibis (2019) due to historical warming. SOLA 2021:17A–002

Kendon EJ, Prein AF, Senior CA, Stirling A (2021) Challenges and outlook for convection-permitting climate modelling. Philos Trans R Soc A3792019054720190547

Kimura F, Kitoh A (2007) Downscaling by pseudo global warming method. Final Rep ICCAP 4346:463–478

Knutson TR, Tuleya RE (2004) Impact of CO2-Induced Warming on Simulated Hurricane Intensity and Precipitation: Sensitivity to the Choice of Climate Model and Convective Parameterization. J Clim 17(18):3477–3495

Knutson T, Camargo S, Chan J, J C Emanuel K Ho C H Kossin J & Wu L, (2020) Tropical cyclones and climate change assessment: Part II: Projected response to anthropogenic warming. BAMS 101(3):E303–E322

Knutson T, Sirutis JJ, Vecchi GA, Garner ST, Morris M-S, Bender Robert A, Tuleya Isaac E, Held M, Villarini G (2013) Dynamical downscaling projections of 21st century Atlantic hurricane activity: CMIP3 and CMIP5 model-based scenario. J Clim 26(17):6591–6617

Knutson TR, Maya VC, Gabriel AV, Jingru ST-LH, Adam JS (2021) ScienceBrief Review: climate change is probably increasing the intensity of tropical cyclones. [Le Quéré Corrine Peter Liss and Piers Forster (ed)] In Critical Issues in Climate Change Science. https://doi.org/10.5281/zenodo.4570334

Kossin J (2021) Tropical Cyclones and Climate Change: What Do We Know? 2021 RA-IV Workshop on Hurricane Forecasting and Warning https://www.publicwmoint/en/events/workshops/ra-iv-workshop-hurricane-forecasting-and-warning-online

Lackmann GM (2015) Hurricane Sandy before 1900 and after 2100. BAMS 96(4):547–560

Lara (2020) The most destructive typhoons in the Philippines. https://www.philstarlifecom/news-and-views/755589-most-destructive-typhoons-ph-typhoon-rolly?page=4

Lee JD, Wu CC (2018) The Role of Polygonal Eyewalls in Rapid Intensification of Typhoon Megi (2010). J Atmos Sci 75(12):4175–4199

Li F, Song J, Li X (2018) A preliminary evaluation of the necessity of using a cumulus parameterization scheme in high-resolution simulations of Typhoon Haiyan (2013). Nat Hazards 92:647–671

Liu M, Vecchi GA, Smith JA et al (2019) Causes of large projected increases in hurricane precipitation rates with global warming. npj Clim Atmos Sci 2(1):1–5

Lynn BH, Healy R, Druyan LM (2009) Investigation of Hurricane Katrina characteristics for future, warmer climates. Clim Res 39(1):75–86

Manganello JV, Hodges KI, Dirmeyer B, Kinter JL, Cash BA, Marx L, Jung T, Achuthavarier D, Adams JM, Altshuler EL, Huang B (2014) Future changes in the western North Pacific tropical cyclone activity projected by a multidecadal simulation with a 16-km global atmospheric GCM. J Clim 27(20):7622–7646

Meehl GA, Senior CA, Eyring V, Flato G, Lamarque J-F, Stouffer RJ, Taylor KE, Schlund M (2020) Context for interpreting equilibrium climate sensitivity and transient climate response from theCMIP6 Earth system models. Sci Adv 6(26), eaba1981

Mittal R, Tewari M, Radhakrishnan C, Ray P, Singh T, Nickerson AK (2019) Response of tropical cyclone Phailin (2013) in the Bay of Bengal to climate perturbations. Clim Dyn 53(3–4):2013–2030

Mori N, Kato M, Kim S, Mase H, Shibutani Y, Takemi T, Yasuda T (2014) Local amplification of storm surge by Super Typhoon Haiyan in Leyte Gulf. Geophys Res Lett 41(14):5106–5113

Müller WA, Jungclaus JH, Mauritsen T, Baehr J, Bittner M, Budich R, Bunzel F, Esch M, Ghosh R, Haak H, Ilyina T (2018) A higher-resolution version of the max planck institute earth system model (MPI-ESM1. 2-HR). J Adv Model Earth Syst 10(7):1383–1413

Murakami H, Wang Y, Yoshimura H, Mizuta R, Sugi M, Shindo E, Adachi Y, Yukimoto S, Hosaka M, Kusunoki S, Ose T, Kitoh A (2012) Future Changes in Tropical Cyclone Activity Projected by the New High-Resolution MRI-AGCM. J Clim 25(9):3237–3260

Nakamura R, Shibayama T, Esteban M, Iwamoto T (2016) Future typhoon and storm surges under different global warming scenarios: case study of typhoon Haiyan (2013). Nat Hazards 82:1645–1681

NDRRMC (2012) National Disaster Risk Reduction and Managament Council (NDRRMC) Update: SitRep No38 re Effects of Typhoon Pablo (Bopha) 25 December 2012 6:00AM https://www.reliefwebint/sites/reliefwebint/files/resources/NDRRMC%20Update%20Sitrep%20No%2038%20re%20Effects%20of%20Typhoon%20Pablo%20Bophapdf

National Oceanic and Atmospheric Administration (NOAA) (2018) National Centers for Environmental Information Global Climate Report – September 2018 https://www.wwwncdcnoaagov/sotc/global/201809

Nayak S, Takemi T (2020) Robust responses of typhoon hazards in northern Japan to global warming climate: cases of landfalling typhoons in 2016. Meteorol Appl 27(5):e1954

NDRRMC (2014) Final Report re: Effects of Typhoon Yolanda (Haiyan) https://www.ndrrmcgovph/attachments/article/1329/FINAL_REPORT_re_Effects_of_Typhoon_YOLANDA_(HAIYAN)_06-09NOV2013pdf

NDRRMC (2018) NDRRMC Update: SitRep No57 re Preparedness Measures: Effects for TY OMPONG as of 0600H06OCT2018pdf https://www.ndrrmcgovph/attachments/article/3437/SitRep_No_57_re_Preparedness_Measures_Effects_for_TY_OMPONG_as_of_0600H_06OCT2018pdf

NOAA (2021) National Weather Service Climate Prediction Center's Cold & Warm Episodes by Season https://www.wwwncdcnoaagov/sotc/global/201809

Parker CL, Bruyère CL, Mooney PA, Lynch AH (2018) The response of landfalling tropical cyclone characteristics to projected climate change in northeast Australia. Clim Dyn 51:3467–3485

Patricola CM, Wehner MF (2018) Anthropogenic influences on major tropical cyclone events. Nature 563(7731):339–346

Radu R, Toumi R, Phau J (2014) Influence of atmospheric and sea surface temperature on the size of hurricane Catarina. Q J R Meteorol Soc 140:1778–1784

Reddy P, Sriram D, Gunthe SS et al (2021) Impact of climate change on intense Bay of Bengal tropical cyclones of the post-monsoom season: a pseudo global warming approach. Clim Dyn 56:2855–2879

Roberts MJ, Camp J, Seddon J, Vidale PL, Hodges K, Vannière B, Mecking J, Haarsma R, Bellucci A, Scoccimarro E, Caron L-P, Chauvin F, Terray L, Valcke S, Moine M-P, Putrasahan D,

Roberts CD, Senan R, Zarzycki C, Ullrich P, Yamada Y, Mizuta R, Kodama C, Fu D, Zhang Q, Danabasoglu G, Rosenbloom N, Wang H, Wu L (2020) Projected future changes in tropical cyclones using the CMIP6 HighResMIP multimodel ensemble. Geophys Res Lett 47(14):e2020GL088662

Sato T, Kimura F, Kitoh A (2007) Projection of global warming onto regional precipitation over Mongolia using a regional climate model. J Hydrol 333:144–154

Schär C, Frei C, Lüthi D, Davies HC (1996) Surrogate climate-change scenarios for regional climate models. Geophys Res Lett 23(6):669–672

Sellar AA, Walton J, Jones CG, Wood R, Abraham NL, Andrejczuk M, Andrews MB, Andrews T, Archibald AT, de Mora L, Dyson H (2020) Implementation of UK Earth system models for CMIP6. J Adv Model Earth Syst 12(4)

Seneviratne SI Zhang X Adnan M Badi W Dereczynski C Di Luca A Ghosh S Iskandar I Kossin J Lewis S Otto F Pinto I Satoh M Vincente-Serrano SM Wehner M Zhou BWeather and climate extreme events in a changing climate Masson-Delmotte V Zhai P Pirani A Connors SL Péan C Berger S Caud N Chen Y Goldfarb L Gomis MI Huang M Leitzell K Lonnoy E Matthews J BR Maycock TK Waterfield T Yelekçi O Yu R Zhou B (Eds) Climate Change 2021: The Physical Science Basis Contribution of Working Group I to the Sixth Assessment Report of the Intergovernmental Panel on Climate Change Cambridge University Press (2021)

Shepherd TG Boyd E Calel RA et al Storylines: an alternative approach to representing uncertainty in physical aspects of climate change. Clim. Change 151 555–571

Sirutis KTR, J J Zhao M Tuleya R E Bender M Vecchi G A Villarini G & Chavas D, (2015) Global Projections of Intense Tropical Cyclone Activity for the Late Twenty-First Century from Dynamical Downscaling of CMIP5/RCP45 Scenarios. J Clim 28(18):7203–7224

Skamarock WC, Klemp JB, Dudhia J, Gill DO, Barker DM, Duda M, Huang X-Y, Wang W, Powers JG (2008) A description of the advanced research WRF version 3 NCAR Technical Note NCAR/TN-475?STR National Center for Atmospheric Research Boulder Colorado

Sugi M, Murakami H, Yoshida K (2017) Projection of future changes in the frequency of intense tropical cyclones. Clim Dyn 49:619–632

Sun Y, Zhong Z, Yi L, Li T, Chen M, Wan H, Zhong K (2015) Dependence of the relationship between the tropical cyclone track and western Pacific subtropical high intensity on initial storm size: A numerical investigation. J Geophys Res: Atmos 120(22):11–451

Sun Y, Zhong Z, Li T, Yi L, Camargo SJ, Hu Y (2017) … & Shi. J Impact of Ocean Warming on Tropical Cyclone Track over the Western North Pacific: A Numerical Investigation Based on Two Case Studies J Geophys Res: Atm 122(16):8617–8630

Takayabu I, Hibino K, Sasaki H, Shiogama H, Mori N, Shibutani Y, Takemi T (2015) Climate change effects on the worst-case storm surge: a case study of Typhoon Haiyan. Environ Res Lett 10(6):064011

Tatebe H, Ogura T, Nitta T, Komuro Y, Ogochi K, Takemura T, Sudo K, Sekiguchi M, Abe M, Saito F, Chikira M (2019) Description and basic evaluation of simulated mean state, internal variability, and climate sensitivity in MIROC6. GMD 12(7):2727–2765

Toumi RR, R and Phau J, (2014) Influence of atmospheric and sea surface temperature on the size of hurricane Catarina. QJR Meteorol Soc 140:1778–1784

Vecchi GA, Delworth TL, Murakami H et al (2019) Tropical cyclone sensitivities to CO2 doubling: roles of atmospheric resolution synoptic variability and background climate changes. Clim Dyn 53:5999–6033

Villafuerte MQ II, Hodges LJCR, K I Cruz F T Cinco T A and Narisma G T, (2021) Sensitivity of tropical cyclones to convective parameterization schemes in RegCM4. Clim Dyn 56(5):1625–1642

Walsh KJE, Camargo SJ, Knutson TR et al (2019) Tropical cyclones and climate change. Trop Cyclone Res Rev 8(4):240–250

Walsh KJ, McBride JL, Klotzbach PJ, Balachandran S, Camargo SJ, Holland G, Knutson TR, Kossin JP, Lee TC, Sobel A, Sugi M (2016) Tropical cyclones and climate change. Wiley Interdiscip Rev Clim Change 7(1):65–89

Wu L, Zhao H, Wang C, Cao J, Liang J (2022) Understanding of the effect of climate change on tropical cyclone intensity: a review. Adv Atmos Sci 39(2):205–221

Xu Z, Han Y, Yang Z (2019) Dynamical downscaling of regional climate: a review of methods and limitations. Sci China Earth Sci 62:365–375

Yamada Y, Satoh M, Sugi M, Kodama C, Noda A, Nakano T, M & Nasuno T (2017) Response of tropical cyclone activity and structure to global warming in a high-resolution global nonhydrostatic model. J Clim 30(23):9703–9724

Yamaguchi M, Chan J, Moon C, I J Yoshida K & Mizuta R, (2020) Global warming changes tropical cyclone translation speed. Nat Commun 11(1):1–7

Zhang G, Murakami H, Knutson TR, Mizuta R, Yoshida K (2020) Tropical cyclone motion in a changing climate. Sci Adv 6(17):eaaz7610.